NAA-SR-3573
REACTORS-POWER
64 PAGES

EVALUATION OF CALANDRIA, THIMBLE, AND CANNED-MODERATOR CONCEPTS FOR SODIUM GRAPHITE REACTORS

By
G. L. REED

ATOMICS INTERNATIONAL

A DIVISION OF NORTH AMERICAN AVIATION, INC.
P.O. BOX 309 CANOGA PARK, CALIFORNIA

CONTRACT: AT(11-1)-GEN-8
ISSUED: JUNE 10, 1960

DISTRIBUTION

This report has been distributed according to the category "Reactors-Power" as given in "Standard Distribution Lists for Unclassified Scientific and Technical Reports" TID-4500 (15th Ed.), August 1, 1959. A total of 620 copies was printed.

CONTENTS

TABLES

FIGURES

FIGURES

ABSTRACT

In a sodium-cooled, graphite-moderated reactor, the sodium and graphite must be kept separated. In the designs for the Sodium Reactor Experiment[1] and Hallam Nuclear Power Facility,[2] each moderator and reflector element is shown as individually canned. In the continuing effort to improve the neutron economy and lower the capital costs of sodium graphite reactors, several other methods of separating the sodium and graphite have been investigated. Both the "calandria" and "thimble" reactors have been given serious consideration as alternates to the "canned-moderator".

An analysis including nuclear, heat transfer, and economic comparisons has been made of the three SGR concepts.

Based upon neutron economy and feasibility of core fabrication, the calandria concept appears to offer the greatest potential for improvement in SGR design. The thimble concept provides some improvement in neutron economy but introduces numerous problems requiring developmental work.

I. INTRODUCTION

Sodium-cooled, graphite-moderated reactors combine the superior heat transfer properties of sodium with the low cost, low neutron-absorption characteristics of graphite. Liquid-metal coolants, primarily sodium, have been used successfully in several nuclear reactors, including the Experimental Breeder Reactor and the Submarine Intermediate Reactor. Graphite has been extensively used as a moderator and reflector in experimental and research reactors. Graphite was used in the large plutonium production reactors at Hanford, Windscale, and Calder Hall. The first sodium-cooled, graphite-moderated reactor was the Sodium Reactor Experiment (SRE). The Hallam Nuclear Power Facility (HNPF), under construction by the AEC at Hallam, Nebr. also utilizes the advantages of sodium as a coolant and graphite as a moderator.

One of the problems associated with a sodium-cooled, graphite-moderated reactor is the incompatibility of the two materials. Sodium in direct contact with porous graphite fills the void spaces in the material and causes swelling and distortion. In addition, the absorbed sodium in the moderator significantly contributes to neutron poisoning in the reactor. Carburization of the stainless steel in the primary coolant loop could occur at high temperatures if excessive carbon, from the moderator, became dissolved in the sodium coolant stream.

The objectionable effects caused by sodium in direct contact with graphite have required the design of reactor cores which physically separate the two materials. The SRE and HNPF designs feature a "canned moderator" concept. In this design, graphite logs are machined into hexagonal prisms which are completely enclosed by a thin metal container. In the case of the SRE, the prisms have axial, cylindrical holes through the center of the logs for the process tubes, which normally contain fuel elements. Sodium coolant passes through these tubes and around the fuel elements. The tubes are welded to the top and bottom surfaces of the graphite container material. Over 50 such cans are stacked adjacent to one another to form the active core of the reactor. Additional cans without center-process tubes surround the active core area and form the reflector region. The HNPF core design is basically similar to that of the SRE except that the hexagonal graphite logs are scalloped along the edges, and canned with stainless steel sheet. When stacked together, three scalloped corners form a cylindrical hole in which process channels for fuel and control-rod thimbles are located.

Although the problem of separation of sodium coolant and graphite moderator has been satisfactorily solved in the SRE and HNPF by canning of each log, other methods of separating the graphite from the sodium have been investigated, such as the "calandria" and "thimble" reactor concepts.

In the calandria concept, the graphite moderator and reflector are located in a single container. The moderator is pierced by calandria tubes which form the fuel element channels and coolant flow paths.

In the thimble concept, the uncanned moderator and reflector are positioned on the lower grid plate. Thimbles pierce the moderator and form the fuel element channels and coolant flow path. Both the inlet and outlet coolant plenums are above the reactor core. The coolant flows downward from the inlet plenum along the outside of the fuel element. At the bottom of the core, the coolant reverses direction and flows upward through the fuel element to the outlet plenum.

The improvements sought from the different methods for separating the sodium and graphite are (1) better neutron economy, (2) lower fabrication costs, and (3) increased reliability. The objective of this report is to compare nuclear, heat transfer and economic aspects which are intrinsic to the design of three concepts: (1) canned-moderator, (2) calandria, and (3) thimble. From this comparison, the most favorable concept from both a design and an economic standpoint will be determined. Recent developments, such as substitution of UC for UO_2 fuel, will improve the performance of sodium graphite reactors; but will not change the conclusions reached in this concept-comparison.

II. DESCRIPTION OF REACTOR PLANT AND CONCEPTS

A. GENERAL

The power generating station chosen for this comparative evaluation consists of a 296-Mwt Sodium Graphite Reactor and the associated equipment required for generating and delivering steam at 1150 psia, 925°F, to a turbine-generator with a gross capability of 106 Mwe.

The reactor is sodium cooled, graphite moderated, and fueled with slightly enriched uranium dioxide. (This study was initiated at the time when use of oxide was planned for the HNPF; it would no longer be recommended for an SGR.) The reactor core is located in a cavity below the level of the main operating floor of the reactor building. Arrangement of the moderator and reflector elements and method of containment varies with reactor concept. These variations will be described in detail under each concept description. The concentric-cylinder-type fuel elements are suspended from plugs in the loading face shield above the reactor core. The control rods operate in thimbles which are similarly supported. Drive mechanisms for these control units are supported on a carriage over the shield. Refueling is accomplished by a mechanized, shielded cask which is supported from a gantry and which can be indexed to engage the shield plugs.

Some of the more important plant data are shown in Table I.

A sodium heat-transfer system transfers the thermal energy from the reactor core to the steam generators. The system consists of three parallel circuits, each designed to handle 1/3 of the total power. Each circuit consists of a radioactive primary loop which transfers the thermal energy from the reactor core to an intermediate heat exchanger and a nonradioactive secondary loop which transfers the thermal energy from the intermediate heat exchanger to a steam generator and superheater.

Each primary loop includes a variable-speed centrifugal pump and valves for controlling sodium flow. The intermediate heat exchanger is common to both the primary and secondary loops. The secondary loop contains a sodium expansion tank, a variable-speed centrifugal pump, valves, and a steam generator and superheater.

TABLE I

PLANT DATA

Net electrical output	100 Mw
Gross electrical generation	106 Mw
Gross thermal power	296 Mw
Net plant efficiency	33.8%
Steam Feedwater System	
Feedwater heaters	4
Feedwater temperature	408°F
Steam pressure (at turbine throttle)	1150 psia
Steam temperature (at turbine throttle)	925°F
Turbine exhaust pressure	1-1/2 in. Hg abs
Net cycle heat rate	9600 Btu/kwh
Secondary Sodium System	
No. of circuits	3
IHE* outlet temperature	970°F
IHE* inlet temperature	600°F
Total flow rate	9×10^6 lb/hr
Primary Sodium System	
No. of circuits	3
Reactor outlet temperature	1000°F
Reactor inlet temperature	630°F
Total flow rate	9×10^6 lb/hr

*Intermediate heat exchanger

A four-feedwater-heater extraction cycle supplies feedwater to the evaporator at 408°F where it is evaporated at 1250 psia. The steam is superheated to 930°F. All equipment is sized to supply 930,000 lb/hr of steam at 1150 psia, 925°F to the turbine generator.

The turbine generator has a gross capability of 106 Mwe with a turbine exhaust pressure of 1-1/2 in. Hg abs.

Reactor plant instrumentation, other than standard process instrumentation, consists of nuclear instrumentation, sodium instrumentation, plant-control-system instrumentation, plant-protective-system instrumentation, and radiation monitoring system instrumentation. Nuclear instrumentation circuits measure neutron flux over the range starting from source level to full power. Sodium instrumentation measures pressure, flows, temperatures, and levels in the sodium systems. The plant control system operates the reactor plant (adjusts control rods, pump speeds, etc). The protective system consists of alarm, set-back, and scram circuits to safeguard the reactor against malfunction and errors which might otherwise create hazardous conditions. The radiation monitoring system provides for personnel protection, for indication of off-normal conditions, and for the prevention of the release of excessive amounts of radioactive materials to plant environs.

A variety of auxiliary systems are required in the reactor plant. A sodium service system is provided to fill, drain, and flush the sodium heat transfer loops and purify the sodium. A low-temperature auxiliary cooling system cools the biological shields, freeze seals, cold traps, plugging meters, etc. An inert-gas system maintains an inert-gas atmosphere above the sodium in the reactor, storage tanks, etc. A radioactive-vent system controls the release of any radioactive gases. A radioactive-waste system stores, for eventual disposal, all radioactive-liquid-waste materials.

B. COMPARISON OF REACTOR CONCEPTS

1. Canned-Moderator Reactor Concept

The canned-moderator reactor consists of: (1) reactor core including moderator and reflector elements, with the fuel, control, and instrument elements suspended in the moderator region, and; (2) reactor structure including the vessel, thermal shield, and biological shield.

Figure 1 shows a section through the reactor core. The assembly of moderator, reflector, fuel, control, and instrument elements is contained in a stainless steel vessel. Radially outward from the core are a thermal shock liner, reactor vessel, containment vessel, thermal shields, insulation, reactor cavity liner, and foundation concrete. Below the core are a grid plate, the reactor vessel bottom, containment vessel bottom, and the reactor support structure

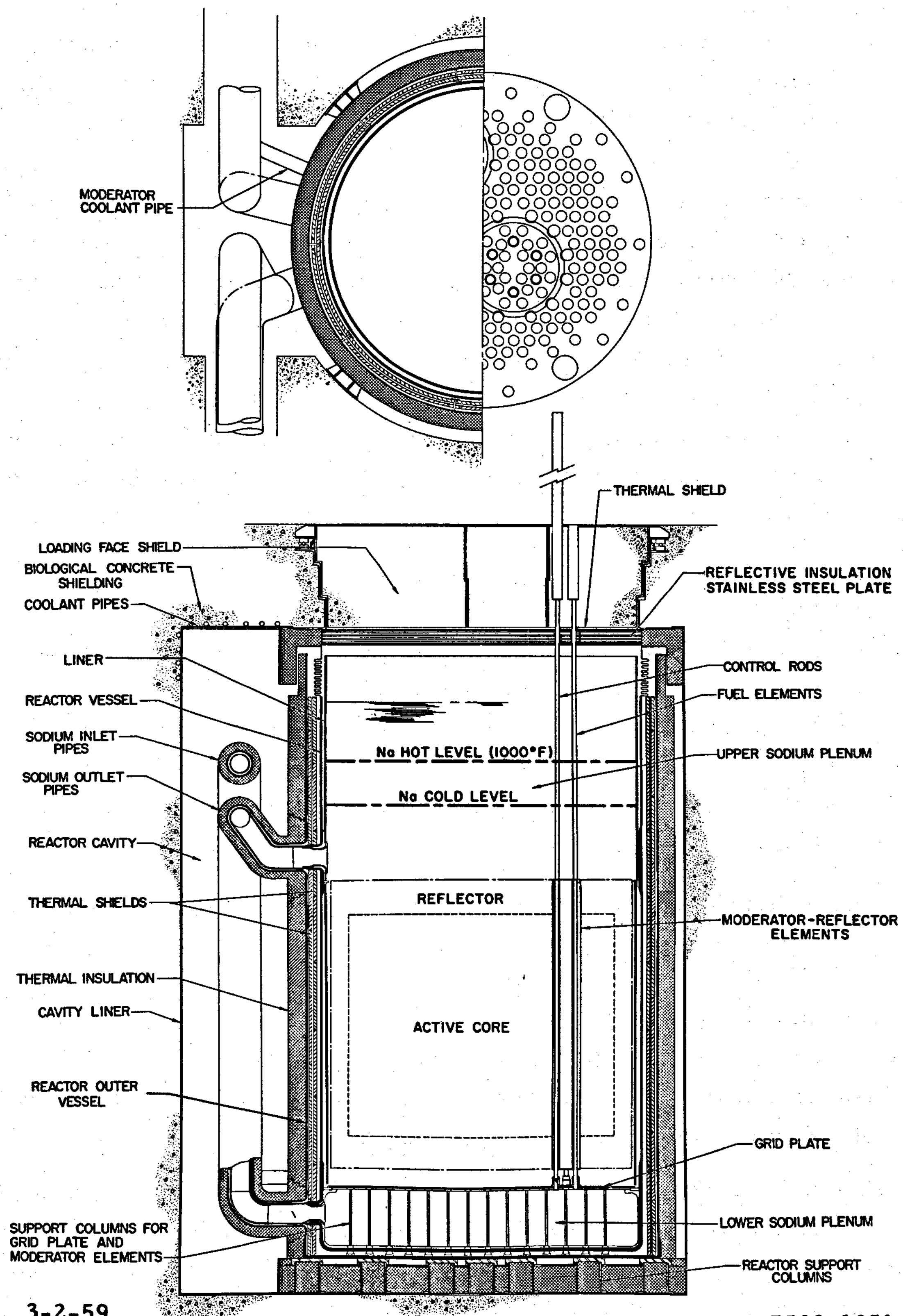

Figure 1. Canned-Moderator Reactor Concept

and foundation concrete. The grid plate supports the moderator and reflector elements and forms the coolant inlet plenum under the core. Above the core are a sodium pool, helium blanket, reflective insulation, and the loading face shield. Sodium is brought to the lower plenum by three pipes which enter the reactor cavity above the core. These are brought down adjacent to the reactor vessel and enter the reactor vessel near the bottom. Sodium is removed from the pool above the core through three outlet pipes attached to the reactor vessel above the core.

a. Reactor Core Components

(1) General

The core consists of closely packed hexagonal prisms of steel-clad graphite with circular corner scallops (moderator and reflector cans) and operating elements suspended in process channels formed by three adjoining scallops. The main flow of sodium coolant is directed up through these channels in Zircalloy-2 process tubes containing the uranium oxide element. Short flow tubes, built into the grid plate, direct the coolant flow to the fuel elements. Piston-ring seals between the flow tubes and the fuel element process tubes prevent excessive coolant leakage to the moderator-coolant areas. Control and instrument elements are interchangeable with fuel elements, but block the grid-plate tube with piston-ring-sealed solid plugs. A parallel coolant system brings about 6% of the sodium flow to a plenum formed by the grid plate and the bottoms of the moderator and reflector cans. This sodium flows upward through gaps between moderator cans and around the outside of elements suspended in the process channels. Heat exchange, through the fuel element process tube to the moderator coolant, assists in maintaining uniform temperature across the core structure.

(2) Moderator and Reflector Elements

Figure 2 shows a cutaway isometric and a simplified section of a moderator element.

The moderator element is a canned-graphite log, hexagonal in cross-section, with corner scallops. The steel cladding is 0.016-in., Type -304 sheet, and the heads are 0.5-in. thick, Type-304 plate. Bolted to the top head

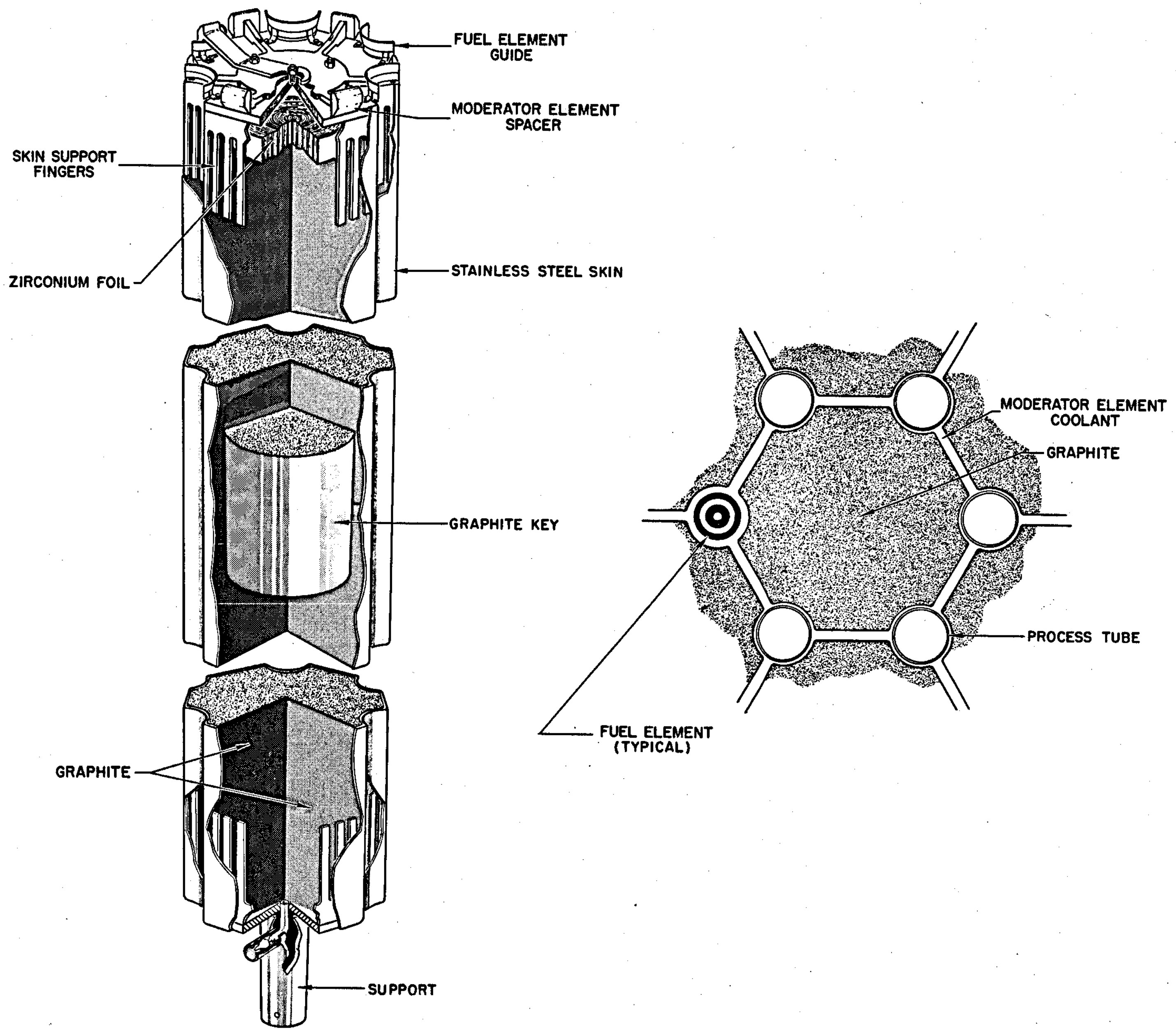

Figure 2. Moderator-Reflector Element for Canned Moderator Reactor Concept

is a spider that acts as a spacer, and a segment of a funnel that guides core elements into the process channels. A pump-out tube and a fitting that engages the support pedestal are at the bottom. Peripheral elements have an additional casting bolted to the top head to engage the core clamps. Inside the top head is a coil of zirconium foil that acts as an absorber for decomposition gases released from the graphite. A formed skirt is welded to the inside face of the heads. This skirt forms a grillage that meshes with machined grooves in the graphite to provide a transition plane for the unsupported cladding, which is otherwise unsupported at the heads due to differential expansion between the graphite and steel.

The reflector region consists of elements identical to the moderator elements. The scalloped corners are filled with circular canned graphite logs to increase the graphite density of this region. These filler elements screw into the bottom grid plate. The element has a flange projection at the upper end that serves as a hold-down device for reflector elements. Unlike the moderator elements, the filler-element cladding does not depend upon the graphite for support. The graphite is undercut in diameter and length to allow for possible swelling. The top head contains a slot to be used for filler element removal.

(3) Fuel Element and Shield Plug Assembly

Figure 3 indicates the general outline of the concentric, hollow-cylinder, uranium dioxide fuel element. The stack of sintered uranium oxide rings is contained between two stainless steel tubes. A helium atmosphere initially fills the gap between UO_2 ring and stainless steel cladding. As burnup proceeds, the helium becomes diluted with fission gases.

The stainless-steel-clad fuel cylinders are supported inside a zirconium-alloy process tube. A mechanical transition is made from zirconium alloy to stainless steel at the upper and lower ends of the process tube. Two piston rings are mounted on the outside of the lower section of the process tube in the lower grid plate. The main coolant flow is channeled from the inlet plenum under the grid plate up through the fuel element. The small leakage through the piston-ring seal goes into the moderator coolant plenum.

The upper steel section of the process tube terminates at a coupling to the shield plug assembly.

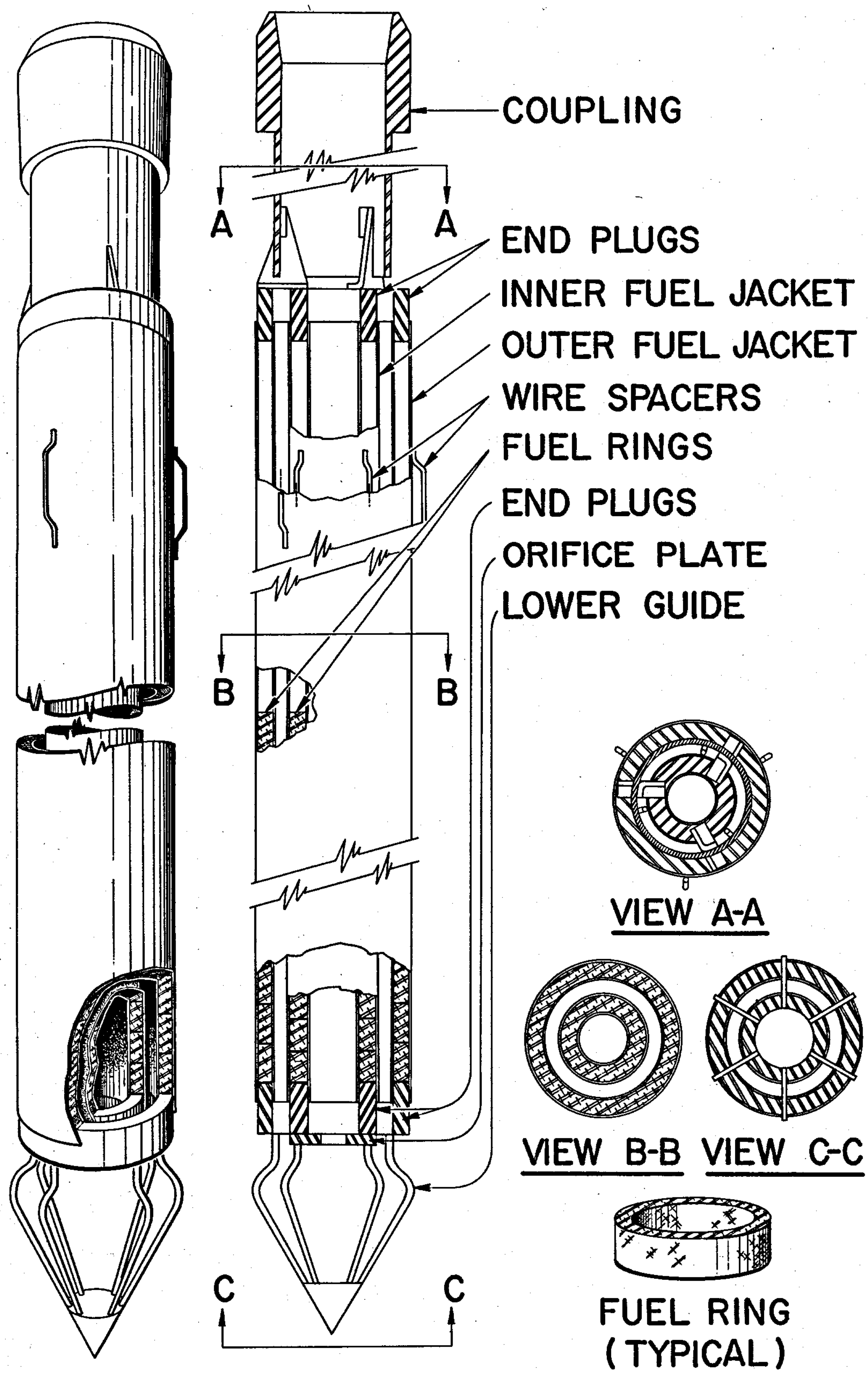

Figure 3. Concentric Cylinder UO_2 Fuel Element

The fuel elements are suspended from the loading face shield by a shield plug assembly. The upper portion of this assembly is a cylindrical steel shell filled with dense concrete and stepped at the midplane for support and to minimize radiation streaming. Two quad-ring seals are used to seal between the shield plug and a similar steel cylinder built into the loading face shield. Thermal insulation is built into the lower end of the plug in a steel-wool-filled section, located vertically to match the reflective plate insulation of the loading face shield. A continuation of the steel cylinder of the plug provides lateral support for the moderator cans and serves as the stationary member of a variable-orifice-control sodium flow through the process channel. The orifice is varied by raising or lowering the mobile member of the variable orifice in the upper section of the process channel. This member is supported by a long hanger tube down the center of the support cylinder. The mechanism used to vary the orifice is a ball-screw unit mounted in the shield plug. A temperature signal for setting flow, as well as for the control and protective systems, is provided by a thermocouple brought through this movable hanger tube and terminating in the sodium channel just above the fuel cylinders.

(4) Control Assemblies

Shim-regulating rods and safety rods occupy corner-channel core positions identical with fuel positions. The absorber section of a rod operates in a helium-filled thimble which penetrates the loading face shield. The thimble extends from the loading face, at reactor floor level, through the reactor core. The lower end of the thimble plugs the opening in the grid plate which is identical with a fuel-coolant opening. The actuator section of the rod is above the loading face floor. Drives are mounted on top of the actuator.

(a) Shim-Regulating Rod Assembly

The shim-regulating rod, shown in Figure 4, consists of an absorber column which is raised and lowered by a ball-nut on a rotating screw. The screw is driven through a gear reduction by an electric motor.

The absorber column is composed of boron-nickel alloy rings stacked on a stainless steel pull-tube. The pull-tube is suspended from pull rods which pass through a shield plug filled with dense concrete. This much of the assembly is contained in a zirconium-alloy thimble, and remains in the reactor when the loading face is cleared for fuel handling operations.

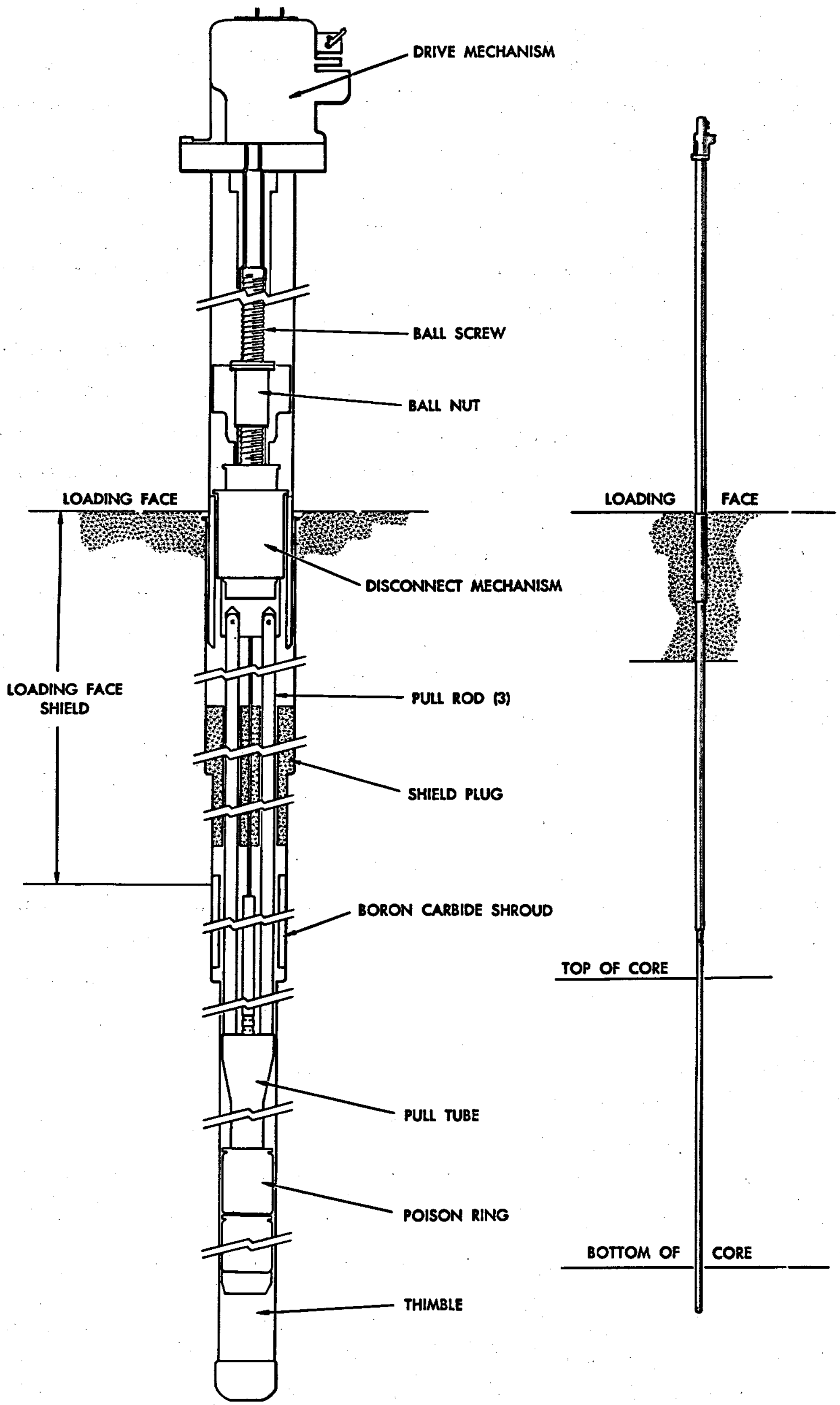

Figure 4. Shim-Regulating Rod

A shroud filled with boron-carbide, which extends from the shield plug to just above the moderator can, reduces the induced activity in the three pull rods, portions of which travel from below to above the shield.

(b) Safety Rod Assembly

The safety rod actuation differs in concept from the shim-regulating rod in that the linear motion is obtained with a chain-and-sprocket system rather than with a ball-nut-and-screw arrangement. This rod is shown in Figure 5.

The absorber section, pull tube, and shield plug are similar to the shim-regulating rod except that the boron-carbide shroud is not used. A gas snubber piston is fixed to the top of the pull rod. The snubber piston is lifted by an electromagnet attached to the end of a chain. The chain passes over the drive sprocket and into a slack well, to a counter-weight sprocket; and then dead-ends at the top of the actuator housing. Cable-leads to the magnet are carried on the chain. The electromagnet is the scram mechanism.

(5) Miscellaneous Core Elements

The miscellaneous core elements include a source, dummy elements, sodium-level indicators, sodium-temperature indicators, and neutron-instrumentation elements. With the exception of the sodium-level indicators, these elements fit any core position and are provided with plugs to close the openings in the grid plate.

The reactor structure is composed of the following major components:

a) loading face shield

b) reactor vessel and internals

c) containment vessel

d) thermal shields and thermal insulation

e) support structure for the reactor vessel and thermal shield

f) cavity liner and gallery diaphram seal

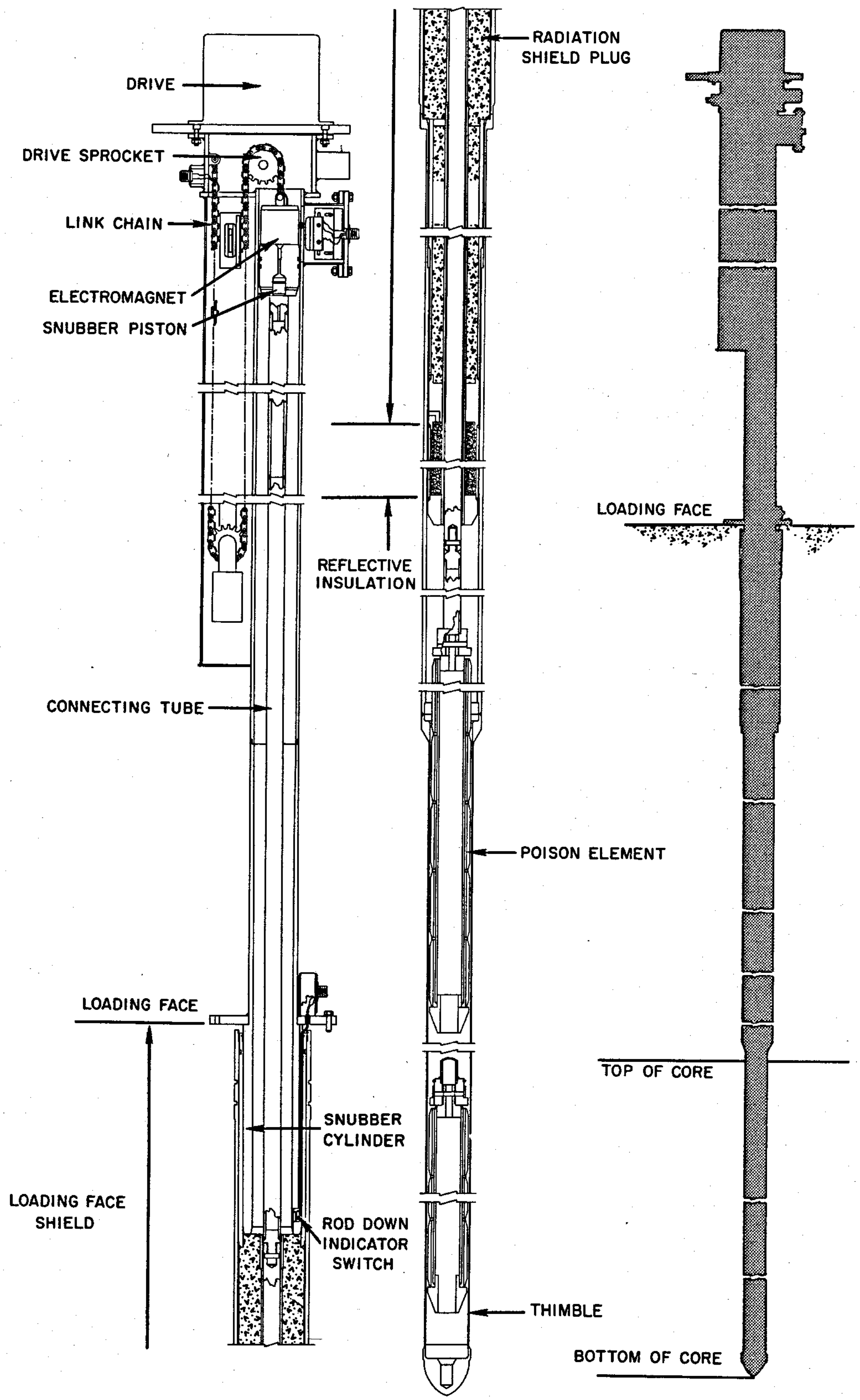

Figure 5. Safety Rod

Detailed descriptions of the reactor-structure components for the three concepts treated in this report are not covered here because in most cases the structures are similar in design and do not greatly affect the technical or economic comparison of the three concepts. Except for dimensions, the structural components for the canned-moderator concept follow very closely the design for the HNPF. Some major differences in reactor structures for the three concepts are covered in the paragraphs below.

The loading face shield is a large, double-stepped, cylindrical plug made of dense concrete encased in steel. In the case of the canned-moderator concept, special features are provided for rotating the loading face shield in order to remove individual moderator cans through one of three small plugs. These features are not required for the thimble or calandria concepts.

A stainless steel reactor vessel with a bellows expansion joint at the top is required in the canned-moderator and calandria concepts to contain the outlet sodium. This tank and a backup containment tank outside the reactor vessel are not required for the thimble concept.

2. Thimble Reactor Concept

In the thimble reactor concept, no canning or containment is required for the graphite moderator and reflector, and the reactor vessel is eliminated. The sodium coolant in the core region is contained in thimbles. Both the inlet and outlet sodium plenum are above the active core region (Figure 6). From the inlet plenum, the sodium coolant flows downward between the thimble and the outer fuel cylinder. At the bottom of the fuel element, the flow is reversed and the sodium flows upward, some of the coolant flowing between the two cylinders and the remainder flowing up the center of the inner cylinder. The coolant overflows the top of the process sleeve into the outlet coolant plenum.

a. Reactor Core Components

The major components of the reactor core are moderator and reflector elements, fuel elements, control elements, and other miscellaneous small core components.

(1) Moderator and Reflector Elements

The moderator and reflector elements are uncanned graphite logs with a hexagonal cross section. The logs are positioned and supported by

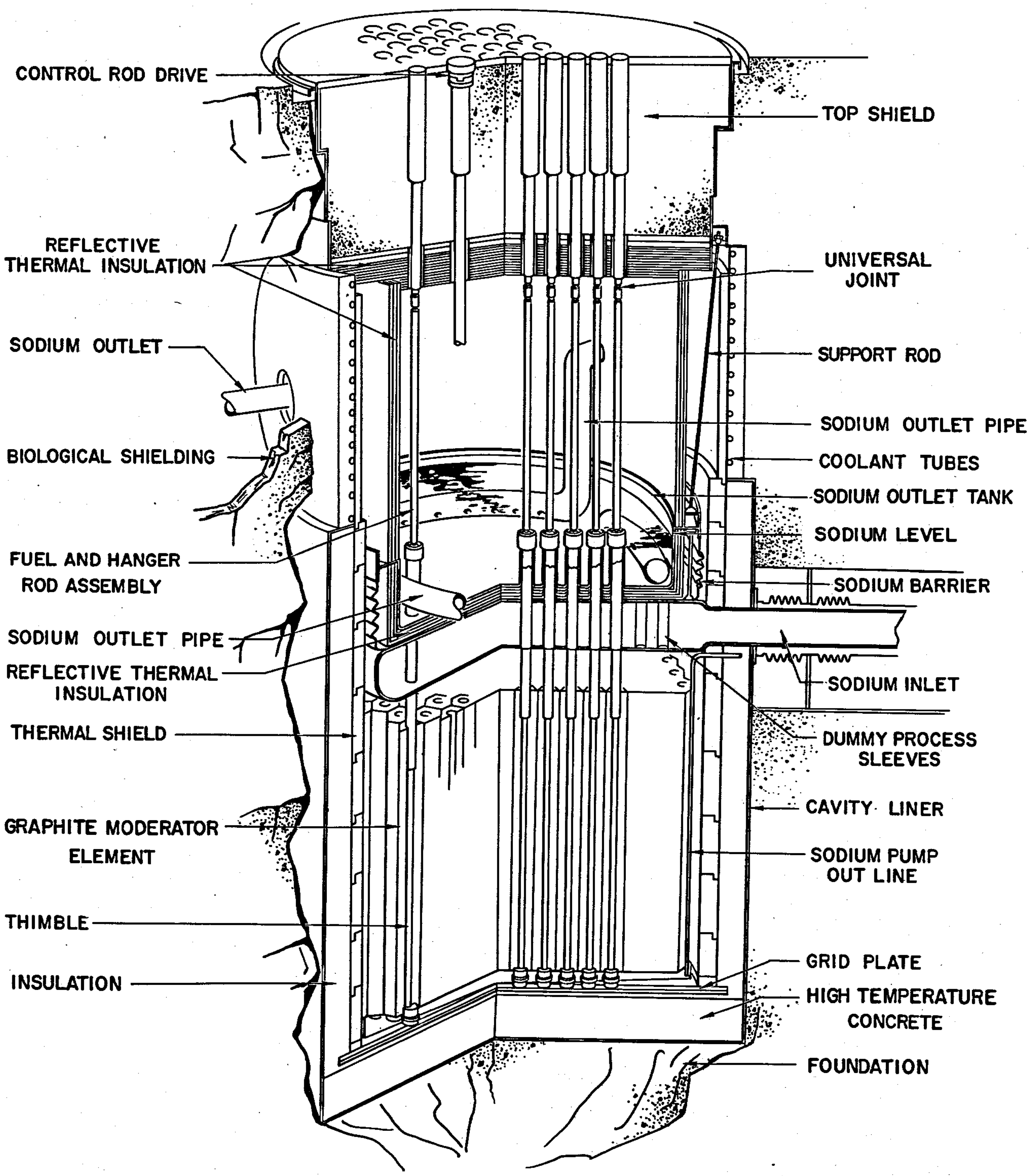

Figure 6. Thimble Reactor

pedestals on the grid plate, which also provides a space for collection of sodium from small leaks. An inert-gas atmosphere is maintained in the graphite region.

In the core region, thin-wall stainless steel thimbles penetrate each graphite log. Each thimble is supported from the bottom of the inlet plenum and is free to expand downward. The bottom of the thimble is capped (see Figure 7). A zirconium liner protects the graphite from sodium leakage.

(2) Fuel Element and Hanger Tube Assembly

The fuel element assembly is similar to the concentric cylinder UO_2 fuel element described previously for the canned-moderator reactor concept. A seal is provided between the outer fuel cylinder and the process sleeve to divert the inlet sodium downward. A bellows is also required in the stainless steel fuel cladding for the outer fuel cylinder, to allow for differential expansion due to the temperature difference between the outer and inner cladding tubes. A universal joint is provided in the hanger tube to compensate for radial expansion in the core.

(3) Control Elements and Miscellaneous Small Core Components

The control element assemblies and the miscellaneous small core components are of a design similar to those previously described components for the canned-moderator concept.

b. Reactor Structure Components

Major components of the reactor structure are the loading face shield, coolant inlet and outlet tanks, thermal shield, thermal insulation, grid plate, and cavity liner. Only the coolant inlet and outlet tanks differ markedly from the canned moderator design.

(1) Coolant Inlet and Outlet Tanks

The sodium outlet tank is an open-top, stainless steel vessel. Holes in the bottom of the tank are fitted with sleeves which extend above the sodium surface in the tank. Cylindrical caps covering each sleeve are attached to the top of the lower sodium inlet tank, and allow sodium to overflow from the process channel into the outlet tank. This tank is surrounded by stainless steel plates forming reflective thermal insulation. An inert gas atmosphere in the tank is open to the reactor cavity. The tank top fits into the reflective insulation in the

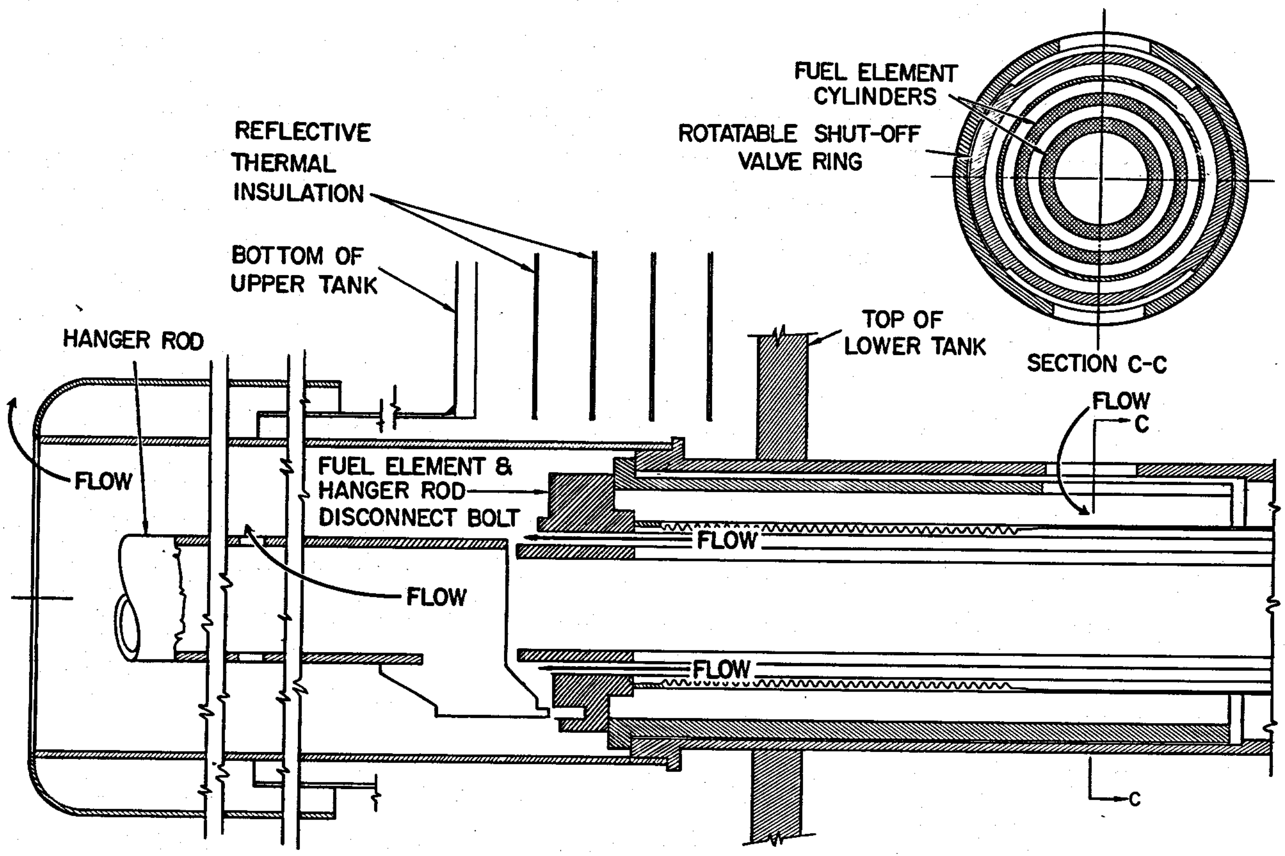

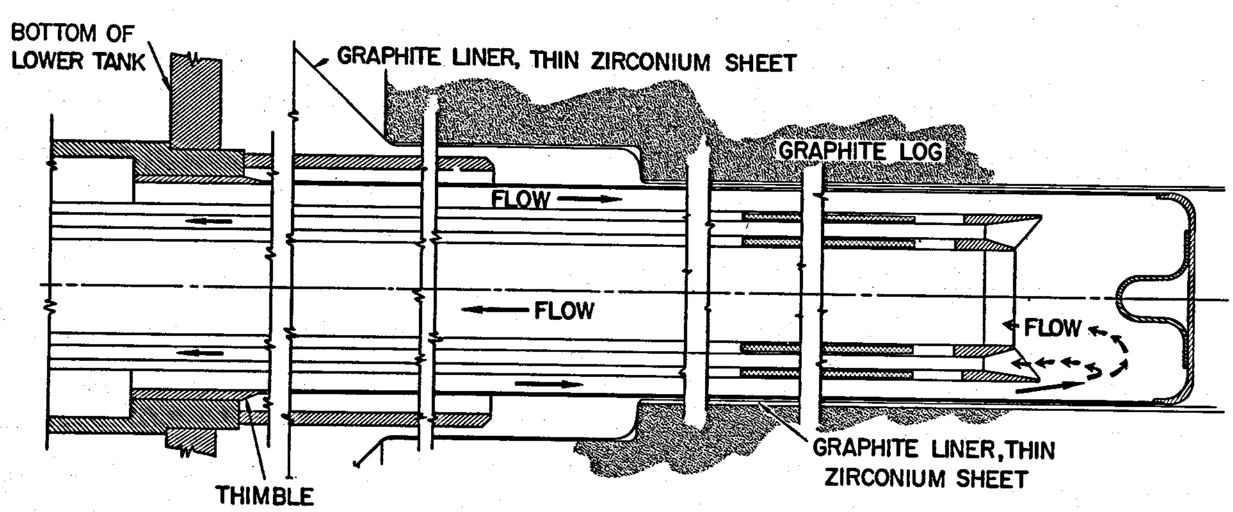

Figure 7. Fuel and Hanger Rod for Thimble Reactor

loading face shield, and any sodium vapor is condensed and returned to the sodium pool. The sodium outlet tank is supported by hanger rods attached to plates embedded in the concrete surrounding the loading face shield.

The sodium inlet tank is a flat-head pressure tank suspended below the outlet tank. Numerous holes, corresponding to the core lattice, are machined in the upper and lower face of the tank. Process sleeves are welded into the holes. Cylindrical caps which cover the sleeves in the upper outlet tank are the upper extensions of these process sleeves. The lower extensions reach down into the core and form the "thimble" in which the fuel element is suspended. Slots in the sleeves permit sodium to flow out of the inlet tank into the thimbles. Rotation of fuel-element and hanger-rod assembly regulates the area of these slots and, therefore, of the sodium flow. Shutoff is possible in case of thimble failure. The inlet and outlet sodium tanks are sealed together at the outer periphery by a ring bellows.

Fabrication of these tanks will require development of remote welding apparatus for welding the upper and lower extensions to the process sleeves.

3. Calandria Reactor Concept

In the calandria reactor concept, graphite moderator and reflector logs are contained in a single container, the calandria tank. In the active section of the core, stainless steel process-tubes extend through the graphite. As in the canned-moderator reactor concept, the primary coolant enters the core from the inlet plenum at the bottom, flows upward past fuel elements in the process-channels, and enters a large pool at the top. Other aspects of reactor core and structure are similar to the canned-moderator concept described previously (see Figure 8).

a. Reactor Core Components

The major components of the reactor core are: (1) calandria vessel containing the graphite moderator and reflector, (2) concentric cylinder fuel elements, (3) control elements, and (4) miscellaneous small core components.

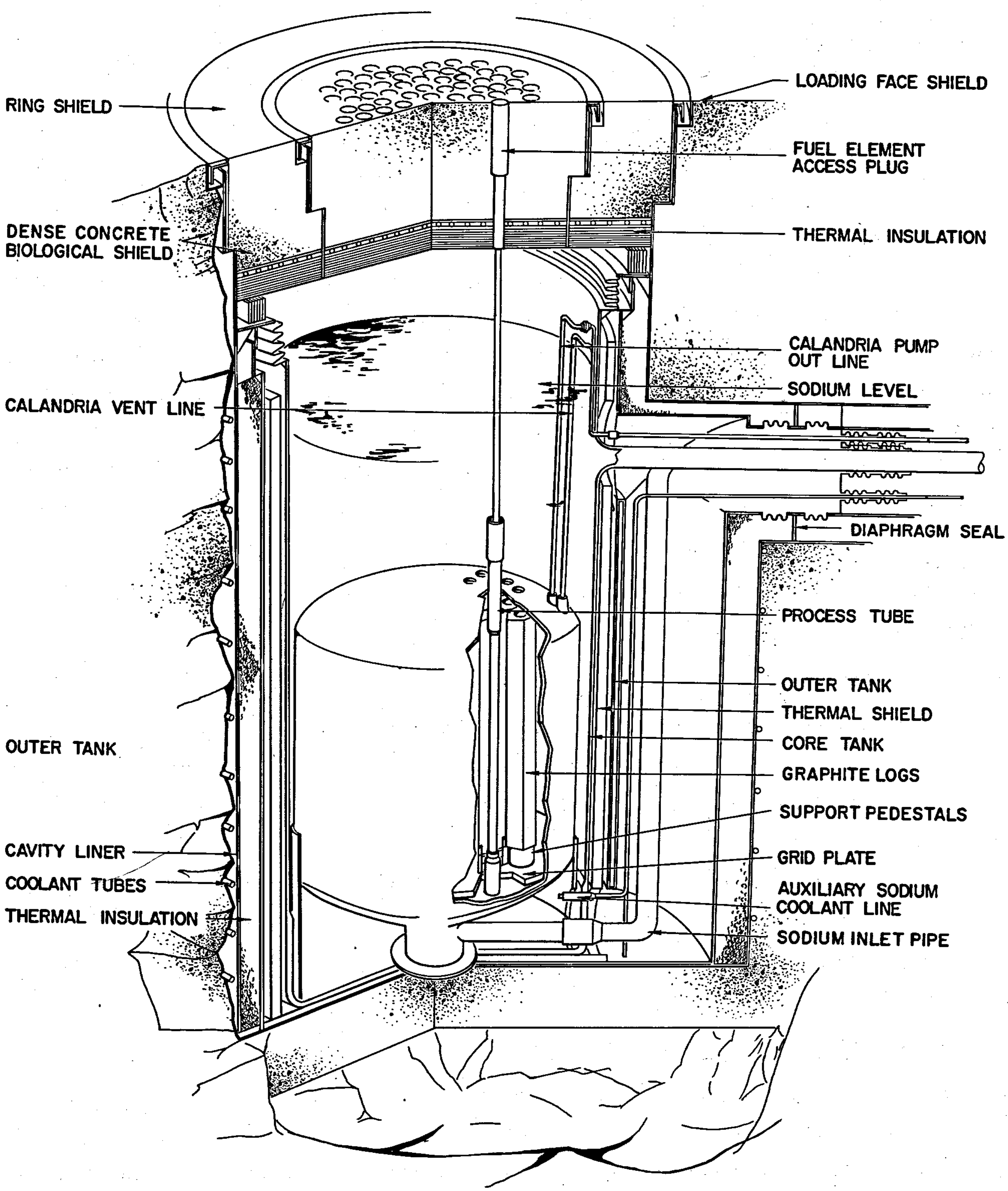

Figure 8. Calandria Reactor

(1) Calandria Vessel

The stainless steel calandria vessel is a cylindrical shell with dished heads. The top head contains nozzles for the process tubes. The bottom head contains nozzles for the three coolant return pipes. The bottom head and grid plate form the lower coolant plenum. The grid plate contains nozzles for the lower end of the process channels.

Graphite moderator and reflector logs are hexagonal in cross section. Logs are positioned and supported by pedestals on the grid plate. The pedestals provide a space for collection of sodium from small leaks. A helium atmosphere is maintained in the vessel around the graphite.

In the core region, stainless steel process-tubes penetrate the graphite logs axially. Each process channel consists of a bottom grid-plate nozzle, process-tube, top head-nozzle, bellows, and bellows guard as indicated in Figure 9. The stainless steel process-tube is welded to the bottom nozzle and extends up to the top head-nozzle. A bellows is provided between process tube and top head-nozzle to allow for differential thermal expansion between calandria vessel and process tube. A guard surrounds the bellows to stagnate sodium and reduce thermal shock.

The calandria tank is installed as a leak-tight vessel. However, a moderate amount of sodium leakage can be tolerated. Such leaking through top head or bellows is excluded from the graphite by a shroud which consists of a conical steel head over the graphite stack and a cylindrical shell of stainless steel at the sides. Process holes in graphite moderator logs are lined with thin-wall zirconium tubes to protect the graphite from any sodium leaks in the process-tube. Sodium which may leak into the calandria vessel is drained to the plenum provided by pedestals supporting the graphite logs. The pump-out line penetrates to this region to permit removal of any sodium which may collect.

Preliminary results of the study of interaction of sodium vapor with graphite indicate that there will be no significant reaction under temperature conditions in the calandria.

(2) Fuel Element Assembly

The fuel-element and hanger-tube assembly for the calandria core is similar in design to that previously described for the canned-moderator

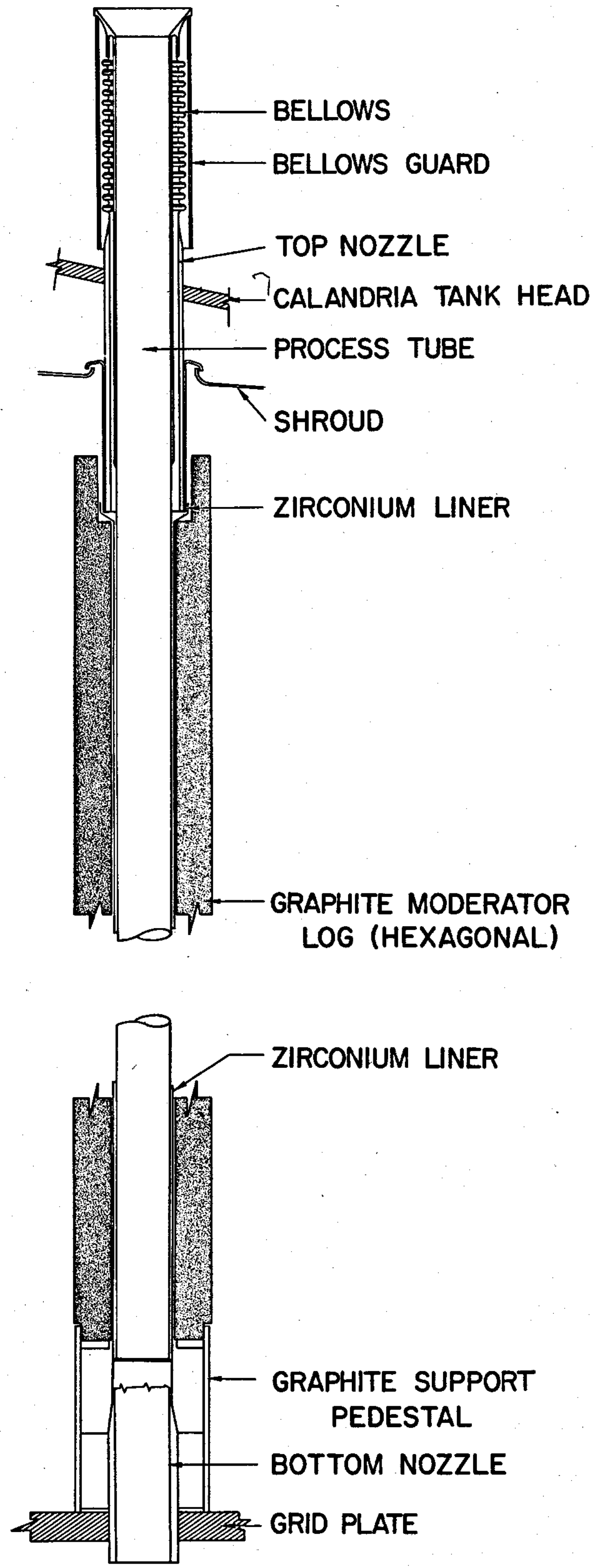

Figure 9. Process Tube for Calandria Reactor

reactor concept (see Figure 4). A variation in design is elimination of the zircalloy process tube required in the canned-moderator design to separate moderator-coolant from higher velocity fuel-coolant.

(3) Control Elements and Miscellaneous Small Core Components

Other components of the reactor core, including control elements and miscellaneous core components, are similar in design to corresponding components in the canned-moderator concept.

III. ANALYSIS

Nuclear and heat transfer studies were conducted to determine, for each concept, a series of reactor core designs of different fuel enrichment, conversion ratio, lattice spacing, and physical size; but with each core design capable of producing 296 Mwe under operating conditions indicated in Table I.

An economic evaluation was conducted to determine the reactor core design which gave minimum power cost for each concept, and to provide a basis for comparison of concepts.

A. NUCLEAR ANALYSIS

Two-group theory was used for criticality calculations. Lattice parameters f, ϵ, P, L^2, and τ were calculated in a conventional manner.[3,4]

Maxwellian-averaged cross sections were used to obtain thermal neutron reactor constants. Thermal flux cell calculations were performed on the IBM-704 using the I-2 code, a solution to the Boltzman equation by the spherical harmonic method in P_3 approximation. Average group constants were obtained by flux- and volume-weighting.

Each core design was based upon obtaining an excess reactivity of 10% at operating temperature and with equilibrium xenon and samarium poisoning. The reflector savings in all cases were assumed to be 40 cm. Other nuclear data used in the analysis are indicated in Tables II and III.

TABLE II

MATERIAL DENSITIES AND OPERATING TEMPERATURES

	Canned Moderator		Calandria and Thimble	
	Temperature (°C)	Density (P) (gm/cm^3)	Temperature (°C)	Density (P) (gm/cm^3)
Graphite	450	1.634	1000	1.61
UO_2	2680 (max.)	10.0	2680 (max.)	10.0
Stainless steel	435	7.72	435	7.72
Sodium	435	0.845	435	0.845

TABLE III

AVERAGE MICROSCOPIC CROSS-SECTIONS (THERMAL NEUTRON)

Material	Canned Moderator			Calandria and Thimble		
	σ_f(barns)	σ_a(barns)	σ_s(barns)	σ_f(barns)	σ_a(barns)	σ_s(barns)
U^{235}	300	360	10.0	222	270	10.0
U^{238}	-	1.53	8.3	-	1.17	8.3
Oxygen	-	Negligible	4.2	-	Negligible	4.2
Graphite	-	0.002905	4.8	-	0.002185	4.8
Stainless steel	-	1.66	9.76	-	1.25	9.76
Sodium	-	0.2825	3.5	-	0.2125	3.5

Variations in core diameter with lattice spacing for various fuel enrichments in canned-moderator, thimble, and calandria-reactor core-concepts are indicated in Figures 10, 11, and 12. Variations in initial conversion ratios with lattice spacing and fuel enrichment are indicated in Figures 13 and 14.

B. HEAT TRANSFER ANALYSIS

Heat transfer calculations for the concentric UO_2 fuel elements were made, based upon operating conditions indicated in Table I (see appendix for derivation of equations). These simplifying assumptions were made: (1) Heat generation was uniform through any cross section of the fuel element and; (2) Each fuel element was properly orificed to obtain uniform outlet coolant temperature, not only from each fuel element channel, but also from each separate coolant path through the fuel element. Properties of materials significant to heat transfer studies are indicated in Table IV.

In studies involving the thimble concept, thermal conductivity of UO_2 was assumed constant at 0.9 Btu/hr-°F-ft because of increased complexity introduced by the double pass of coolant (see Figure 4).

Determination of volumetric heat generation rate in fuel was based upon either a fuel temperature limitation of 4850°F or a pressure-drop limitation

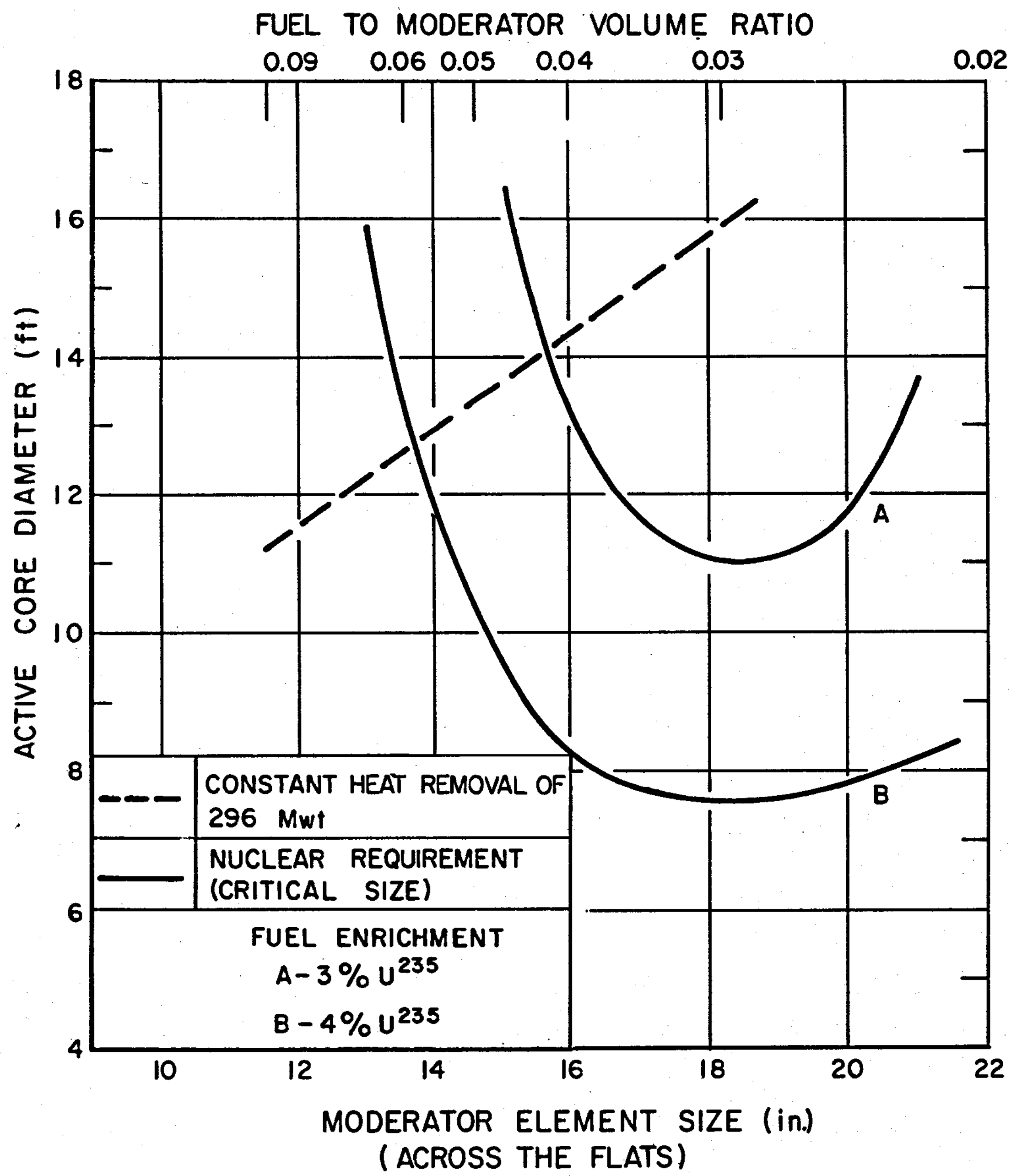

Figure 10. Canned-Moderator Concept: Criticality and Constant Heat Removal Curves for Concentric-Hollow-Cylinder Fuel Element

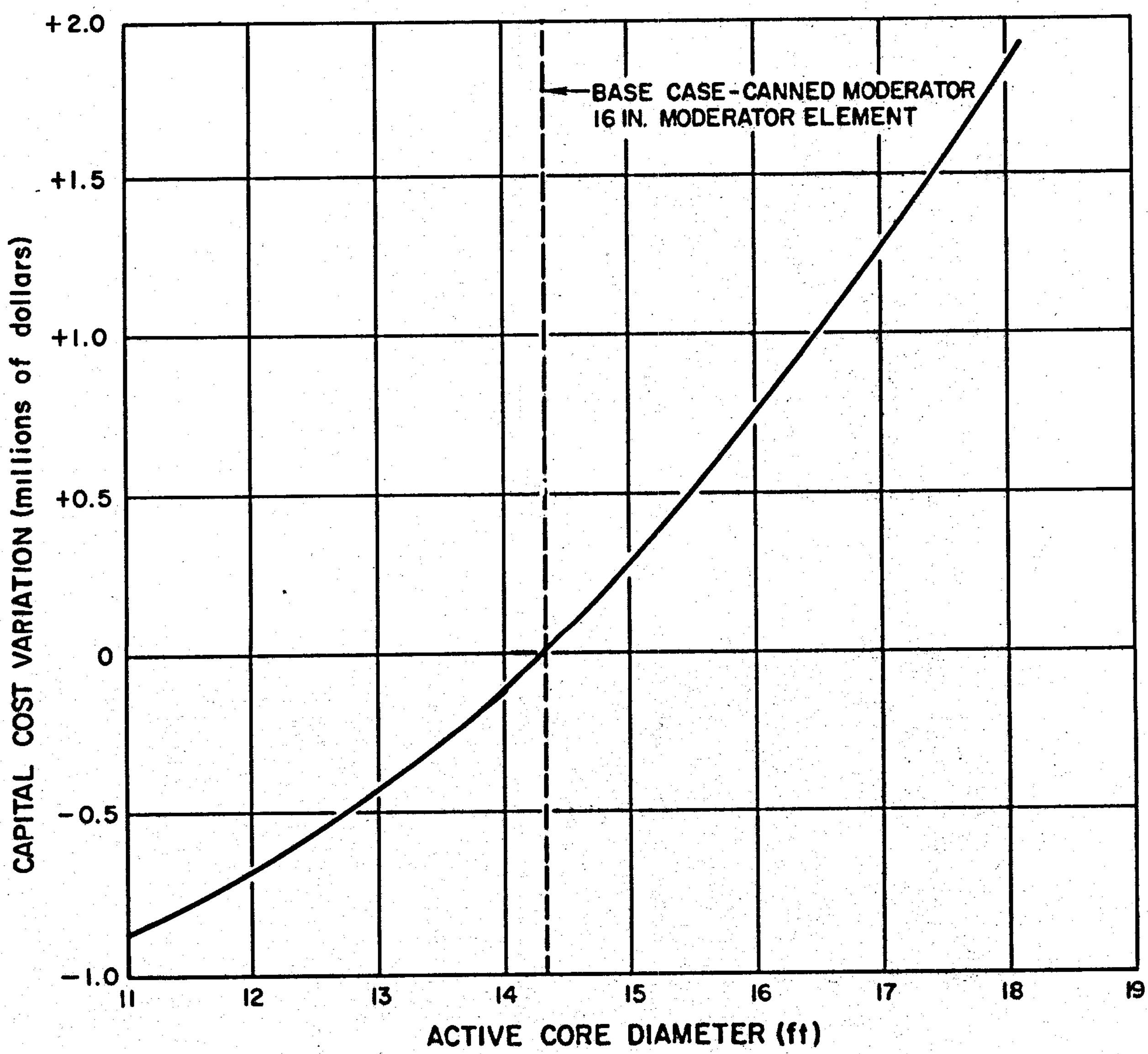

Figure 11. Thimble Concept: Criticality and Constant Heat Removal Curves for Concentric-Hollow-Cylinder Fuel Element

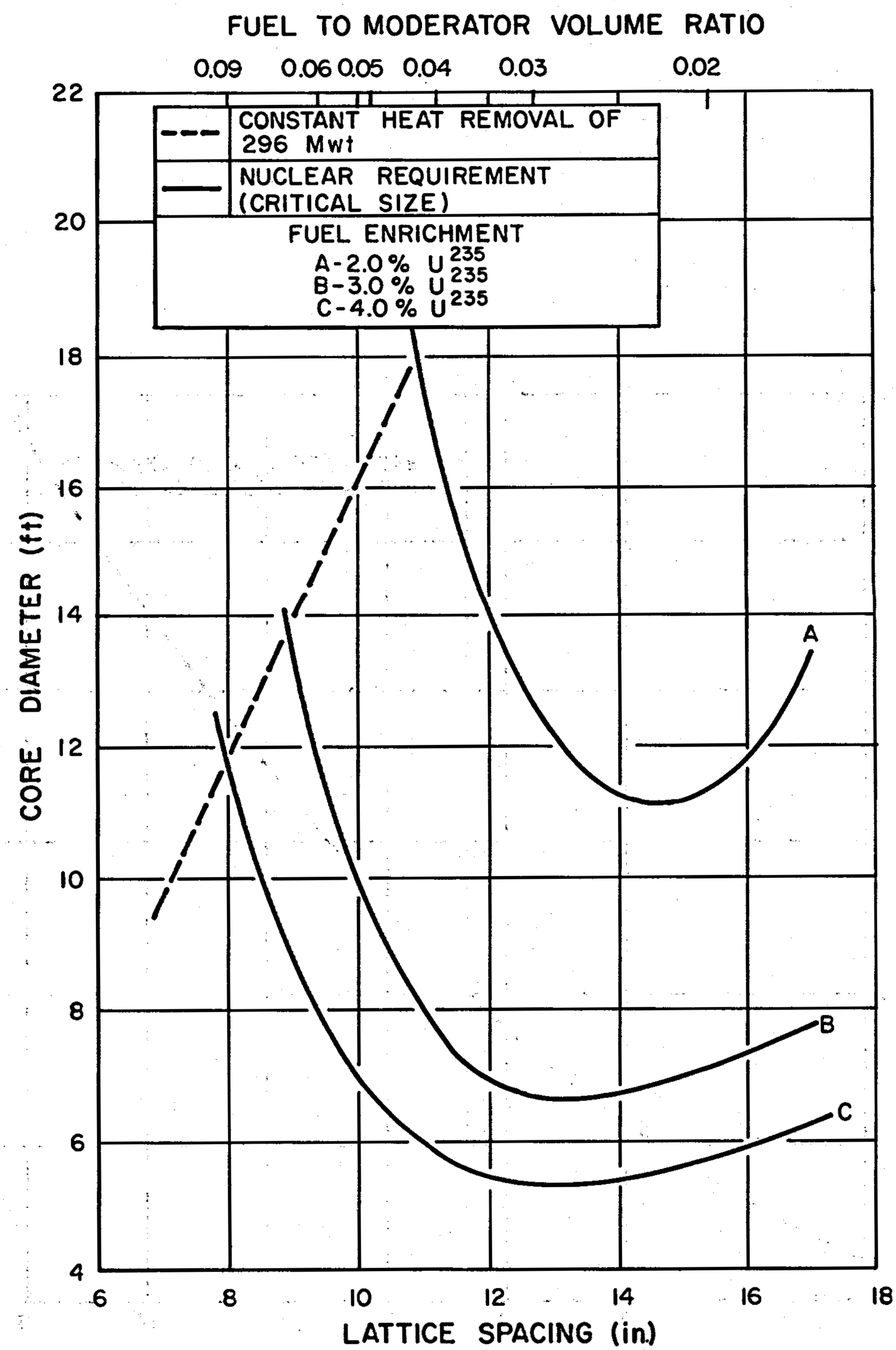

Figure 12. Calandria Concept: Criticality and Constant Heat Removal Curves for Concentric-Hollow-Cylinder Fuel Element

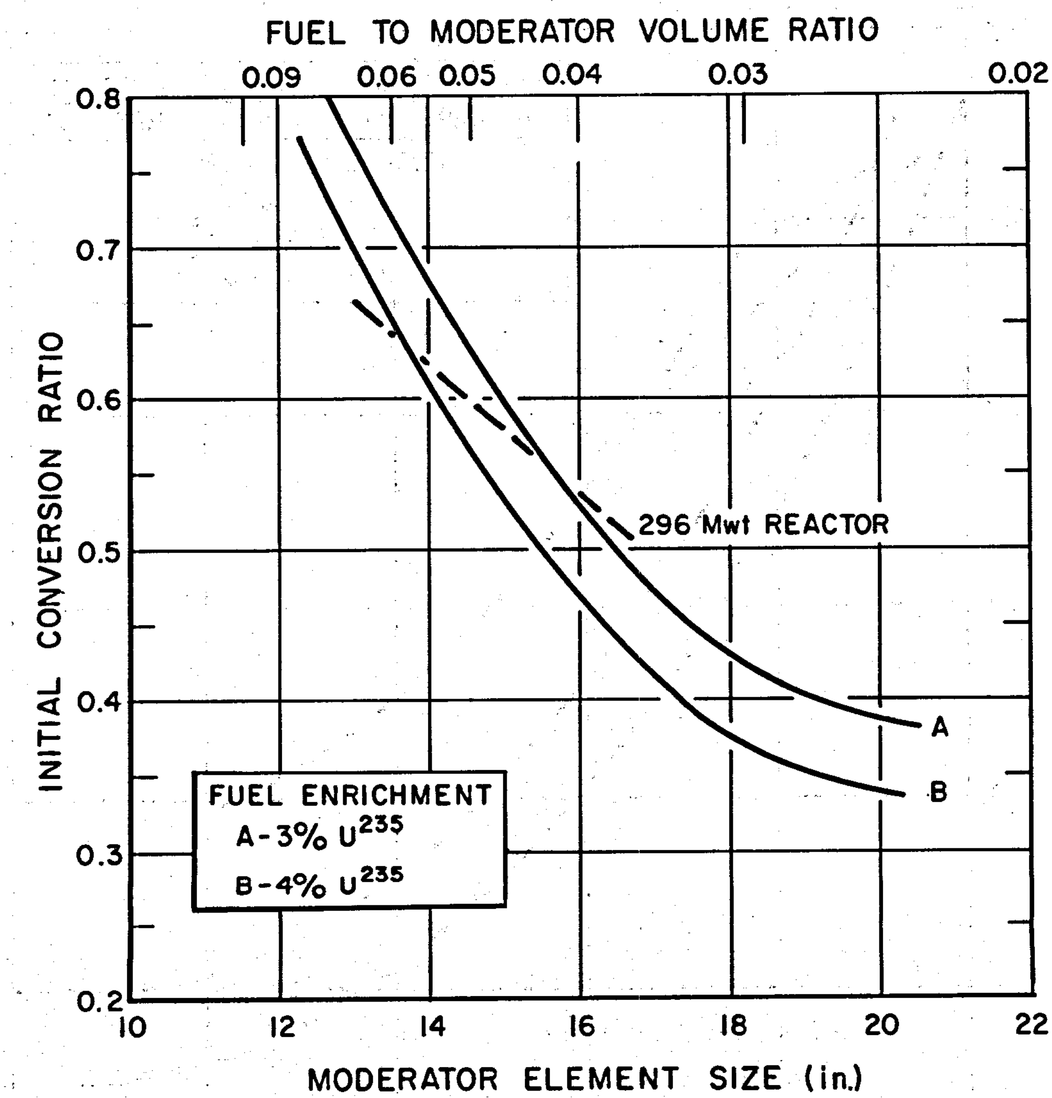

Figure 13. Canned-Moderator Concept: Initial Conversion Ratio for Concentric-Hollow-Cylinder Fuel Element

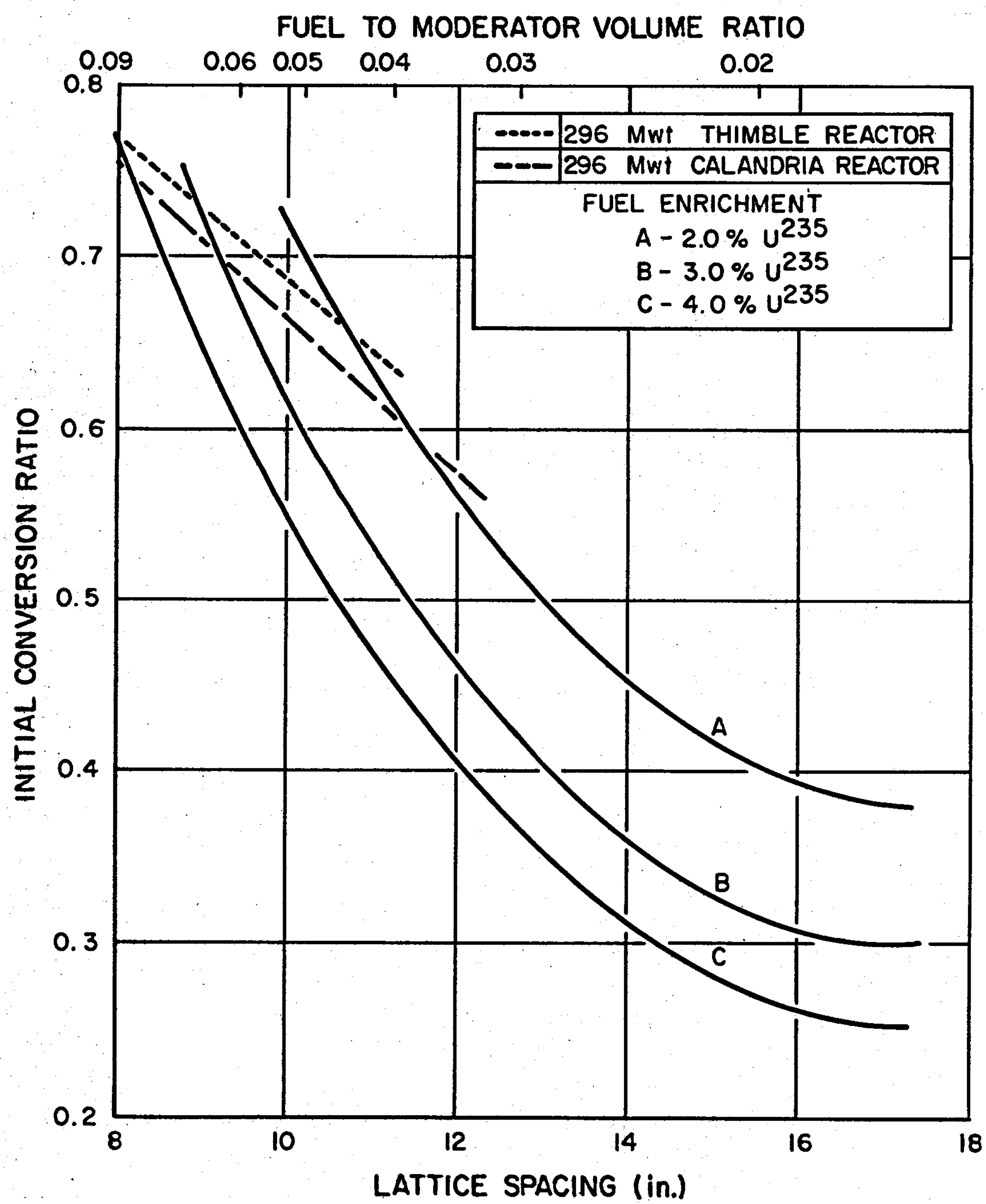

Figure 14. Calandria and Thimble Concepts: Initial Conversion Ratio for Uranium-Dioxide, Concentric-Hollow-Cylinder Fuel Element

TABLE IV

SIGNIFICANT PROPERTIES OF MATERIALS USED

Sodium	
Density (ρ)	53.6 lbs/ft^3
Thermal conductivity (k)	38 Btu/hr-ft-°F
Specific heat (C_p)	0.3 Btu/lb-°F
Stainless steel	
Thermal conductivity (k)	12 Btu/hr-ft-°F
Helium (diluted by fission gases)	
Thermal conductivity (k)	0.05 Btu/hr-ft-°F
Uranium dioxide	
Thermal conductivity (k)	1130 $T^{-0.9}$ Btu/hr-ft-°F* (where T = Absolute temperature °F)

*To facilitate heat transfer calculations for the double-pass, thimble-concept fuel element, a uniform thermal conductivity of 0.9 Btu/hr-ft-°F was assumed for UO_2.

through the core of 25 psi. Assuming uniform heat generation through any cross section of the element, maximum temperature was found to occur at the axial center of the inside cylinder.

Heat generation rate in other fuel sections was considered proportional to thermal neutron flux. Ratio of peak-to-average thermal neutron flux was determined for each case based upon: (1) cell calculation conducted as part of nuclear studies; (2) axial flux in the core varying as a cosine function; (3) radial flux varying as a Bessel function of the zero order, and; (4) a reflector savings of 40 cm.

Variation of core size with lattice spacing for constant heat removal is indicated as dashed-line cross plots in Figures 10, 11, and 12. Each core design is capable of producing 296 Mwt at the operating condition prescribed in Table I. Core size for canned-moderator and calandria concepts was found to be limited by fuel temperature in the range of parameters studied. Core size for the thimble concept was found to be limited by core pressure-drop requirements in the range of parameters studied. The thimble configuration used in this study could have been redesigned to lower pressure drop through the core;

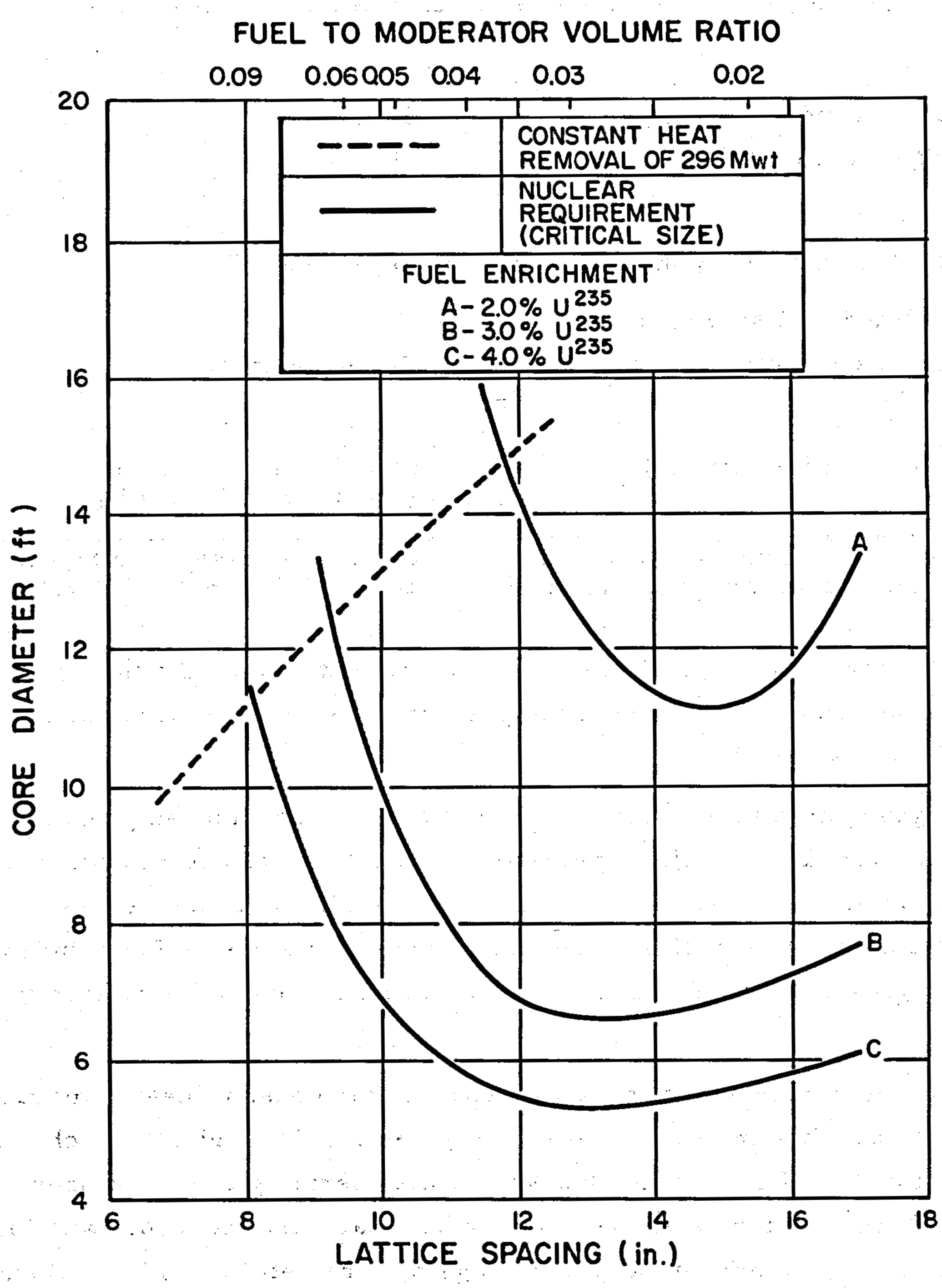

Figure 15. Variation of Total Capital Investment with Diameter of Core-Canned Moderator, Thimble, and Calandria Concepts

however, it is believed that final conclusions pertaining to this concept would not be altered by eliminating pressure-drop restriction.

C. ECONOMIC STUDY

To provide additional basis for evaluation of reactor core concepts, an economic study was conducted which included a determination of variation in capital costs as well as in fuel cycle costs with fuel enrichment, change in reactor size, etc. For comparison purposes a base case or reference has been established, significant data for which are listed in Table V.

TABLE V

REFERENCE DESIGN FOR ECONOMIC STUDY

Concept - canned-moderator reactor
Moderator element size - 16 in. center-to-center spacing
Active core diameter - 14.3 ft
Uranium enrichment - 2.8% U^{235}
Initial conversion ratio - 0.55

All equipment, operating conditions, etc., external to the reactor core and structure remained unchanged throughout the study. Therefore, variation in capital costs is restricted to components which vary with size of the reactor core. These components include moderator, moderator containment, core tank, thermal shield, subsupport structure, cavity liner, top shield including shield plugs, biological shielding, etc.

Variation in total capital investment with reactor core diameter is indicated in Figure 15.

All variations in direct equipment costs and indirect construction costs normally required for design and construction of a power station are included. Although the three core concepts differed somewhat in construction, no difference in capital costs between concepts was apparent for cores of equal size. The cost estimate for the Thimble Reactor Concept assumes prior development of remote welding equipment and techniques. Variation in power generating costs due to

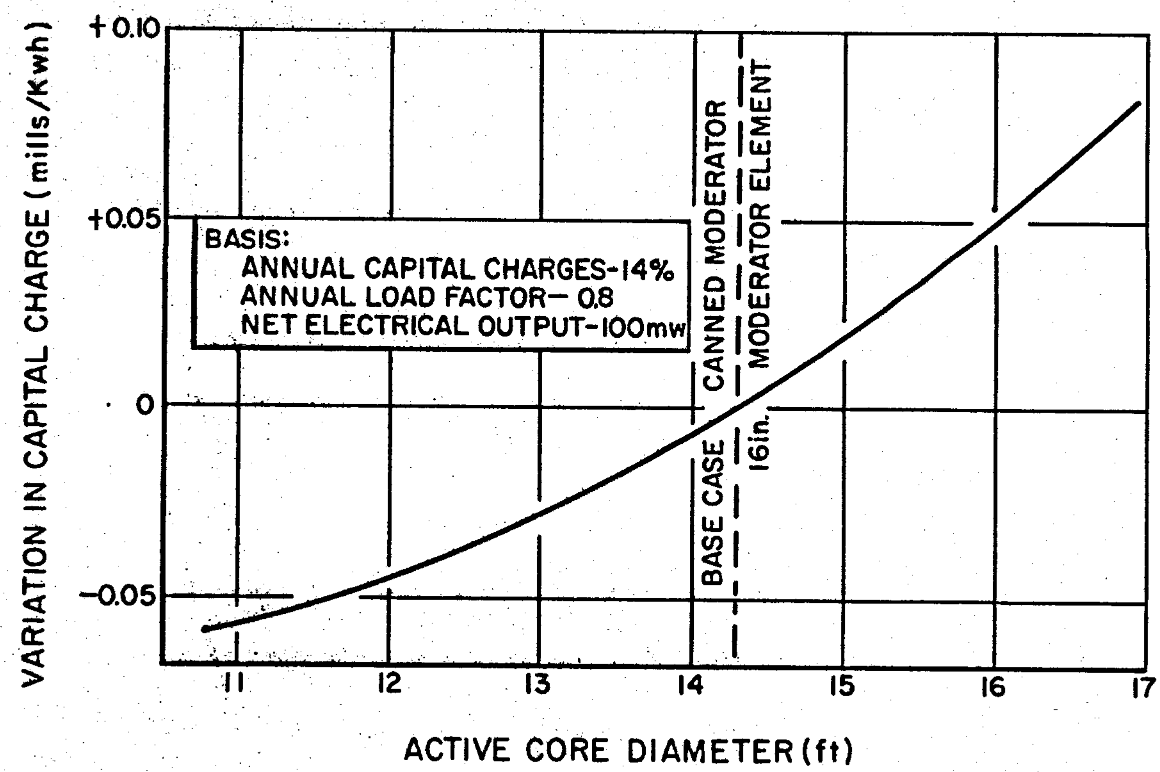

Figure 16. Variation in Capital Charges with Active Core Diameter

variation in capital investment, as indicated in Figure 16, is based upon an annual load factor of 80% and annual capital charge of 14%.

Variation in fuel cycle costs was determined for the various core designs. Fuel cycle costs include the following:

1) Conversion of UF_6 to UO_2 powder (including losses)

2) Forming of UO_2 cylinders and sintering to high density (including losses and recovery of scrap)

3) Assembly of cylinders into complete fuel element

4) Uranium lease charges - in-core and ex-core

5) Shipment of fuel element to reactor site and shipment of spent fuel to reprocessing facility

6) Decladding of fuel and chemical reprocessing to uranyl and plutonium nitrate (including losses)

7) Conversion of uranyl nitrate to UF_6

8) Depletion of U^{235} by fission and nonfission capture

9) Credit for plutonium produced.

All cost estimates are based upon either information published by the AEC or quotations from private fuel suppliers.

In addition, the following bases were established for this study:

1) Average fuel burnup - 10,000 Mwd per metric ton of uranium

2) Net plant thermal efficiency - 33.8%

3) Annual load factor - 0.8.

Variations in fuel cycle costs and total power generation costs are indicated in Figures 17 and 18. All costs are indicated as variations from the base case (canned moderator core, 16-in. moderator elements, 14.3-ft core diameter).

No change in operation and maintenance charges is expected with any variations in core design now considered. Therefore, the net variation in power generating costs will be the sum of the variation in capital charges and fuel cycle costs.

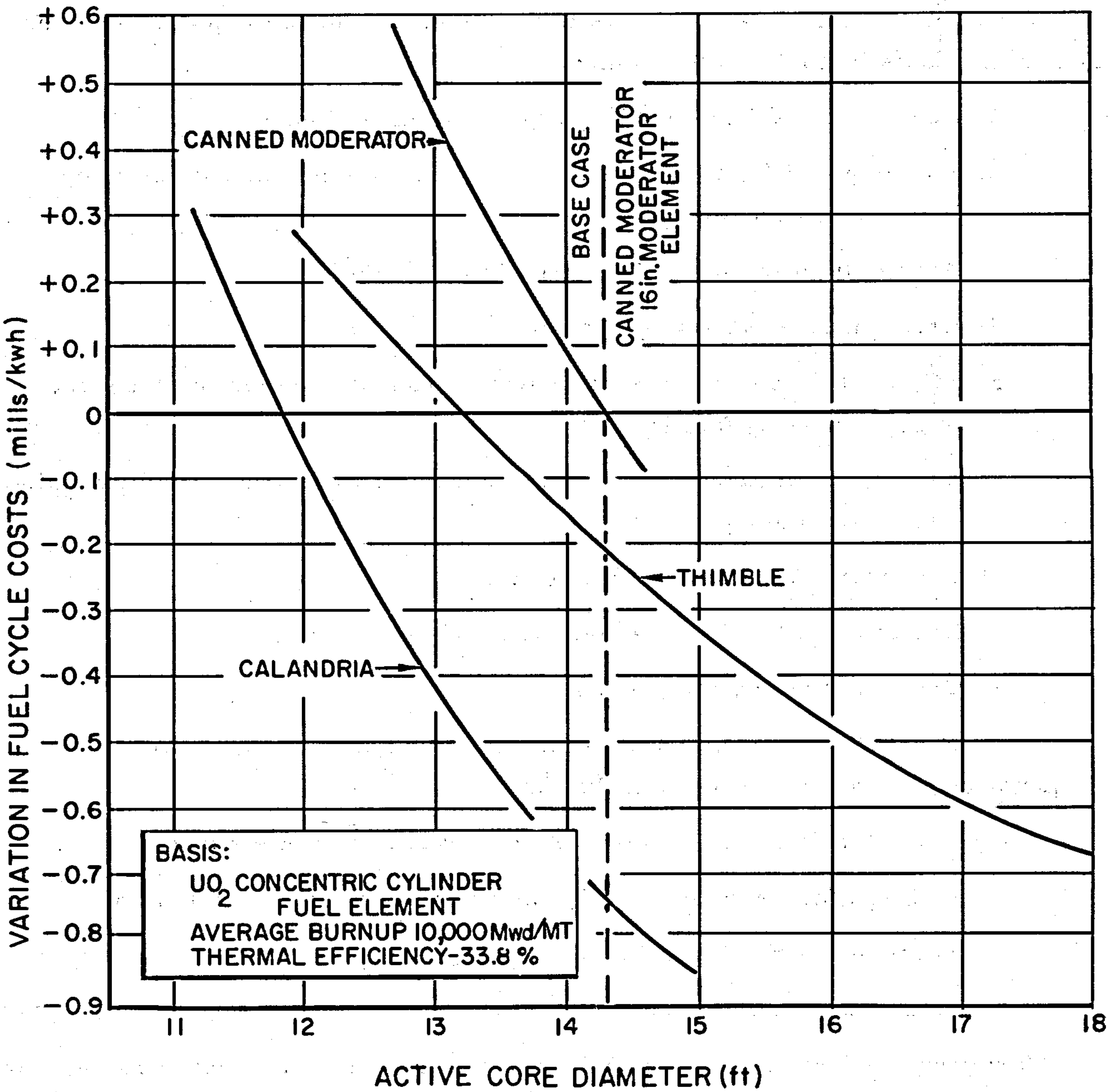

Figure 17. Variation in Fuel-Cycle Costs with Reactor Core Size

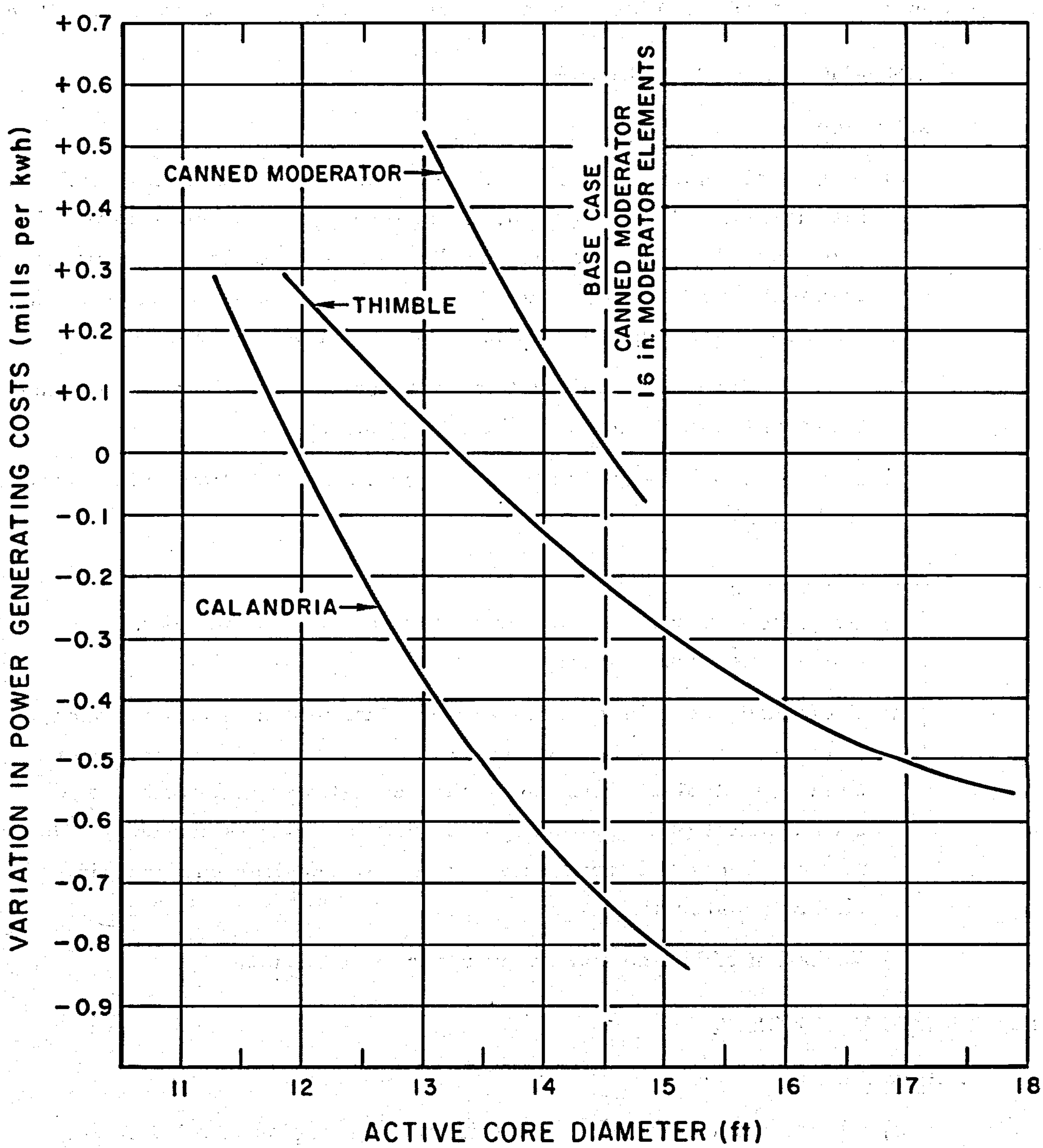

Figure 18. Variation in Total Power Generating Costs with Reactor Core Size

IV. DISCUSSION OF RESULTS AND CONCLUSIONS

Advantages and disadvantages of each of the three SGR concepts considered, i.e., canned-moderator, thimble, and calandria, may be summarized as follows:

A. CANNED-MODERATOR CONCEPT

1. Advantages

   a) Individual containment of small sections of the moderator facilitates installation and replacement, if necessary, of the moderator. To avoid complication of removing the loading face shield for moderator removal, it is necessary to provide for rotation of the shield. Rotatability adds considerably to the cost of the top shield.

   b) Only a relatively small portion of the graphite moderator is saturated with sodium in case of cladding failure.

   c) Feasibility of design has been proven by construction and operation of the SRE.

2. Disadvantages

   a) Graphite-cladding introduces neutron poisons into core and decreases neutron economy.

   b) Probability of failure of moderator containment is highest because of large surface area exposed to sodium, and relative thinness of canning material. Because of the geometry of moderator cans, stress relief (such as through use of a bellows) is difficult. Thermal gradients and transients can lead to buckling and cracking of cladding material.

   c) Variation of lattice spacing in a core is difficult.

B. THIMBLE CONCEPT

1. Advantages

   a) Cladding and structural material in core region is minimized, improving neutron economy and reducing fuel costs.

b) Small sodium leaks into moderator region can be tolerated.

c) Variation of lattice spacing in the core is feasible.

2. Disadvantages

a) Double-plenum tanks in which process tubes are installed present fabrication and installation problems.

b) Natural convection cooling of the fuel elements is difficult to achieve. Removal of decay heat would be more difficult in case of loss of coolant pumping.

c) A major rupture of thimble or plenum tank would necessitate replacement of the entire core. This would be a major undertaking, requiring the removal of both coolant plenums.

d) Provision for differential thermal expansion of fuel element cladding is necessary because of difference in coolant temperature on inner and outer surfaces.

e) Pressure drop through core is considerably increased by double pass of coolant. Pumping power is therefore increased. Power density in fuel may be limited by core pressure drop, and freedom is restricted in selection of fuel element geometry.

f) Graphite temperatures are high since the only means for heat removal is by conduction to the thimble. This leads to impairment of neutron economy, since neutron yield from U^{235} and Pu^{239} decreases with temperature.

C. CALANDRIA CONCEPT

1. Advantages

a) Structural and cladding material in core is minimized – highest neutron economy – lowest fuel-cycle costs.

b) Small sodium leaks into moderator region can be tolerated.

c) Variation of lattice spacing in core is feasible.

2. Disadvantages

a) A major rupture in calandria tube or moderator containment vessel would require replacement of calandria. This would necessitate removal of loading face shield and a rather heavy and bulky calandria.

b) Provision for differential thermal expansion of each calandria tube is required.

c) Graphite temperature is high, reducing the potential gains in neutron economy.

D. CONCLUSIONS

Operating experience is currently available only on the canned-moderator concept. A small calandria has been built to establish fabrication techniques, but no tests have been conducted. Selection of the best of these three concepts must therefore be made primarily on the basis of analytical work presented in this report.

With these qualifications, the calandria concept appears at present to be the most attractive of the three. It has the neutron economy advantage of the thimble concept without the high pressure drop, restrictions on fuel geometry, and complicated cooling-system structure of the thimble reactor. Poorer neutron economy and inherently greater probability of sodium leaks into graphite make the canned-moderator reactor somewhat less attractive.

The calandria concept should be tested, particularly with regard to integrity of the bellows or other stress-relieving fitting required on each process tube. The next experimental SGR should incorporate a calandria core in order to obtain operating experience with this concept.

APPENDIX – DERIVATION OF HEAT TRANSFER EQUATIONS

A. DOUBLE-CONCENTRIC-CYLINDER FUEL ELEMENT – ONCE-THROUGH COOLANT FLOW

Calculation of thermal output consists of solving the general equation of heat conduction with internal sources in cylindrical coordinates.

$$\frac{1}{r}\frac{d}{dr}\left(kr\frac{dt}{dr}\right) = -Q \qquad \ldots(1)$$

Using the variable conductivity coefficient for UO_2 given in Table IV, solution of Equation 1 for a single fuel tube is:

$$1.13 \times 10^4 \left(T_m^{0.1} - T_{s_b}^{0.1}\right) = \frac{Q_o}{4}\left[b^2 - r_1^2 + r_1^2 \ln\left(\frac{r_1}{b}\right)^2\right] \qquad r_1 < r < b, \qquad \ldots(2a)$$

$$1.13 \times 10^4 \left(T_m^{0.1} - T_{s_a}^{0.1}\right) = \frac{Q_o}{4}\left[a^2 - r_1^2 + r_1^2 \ln\left(\frac{r_1}{a}\right)^2\right] \qquad a < r < r_1, \qquad \ldots(2b)$$

where

s and b are inside and outside radii as shown in Figure 19; r_1 is the radius at which maximum fuel temperature occurs.

If surface temperatures T_{s_a} and T_{s_b} are assumed equal, then Equations 2a and 2b can be solved for r_1,

$$r_1^2 = \frac{b^2 - a^2}{\ln\left(\frac{b}{a}\right)^2} \; . \qquad \ldots(3)$$

The heat transfer rate through the bond, cladding, and coolant film per foot of fuel element is

$$q = \left(T_{s_b} - T_f\right)\left(a + b\right) 2\pi (1) U, \qquad \ldots(4)$$

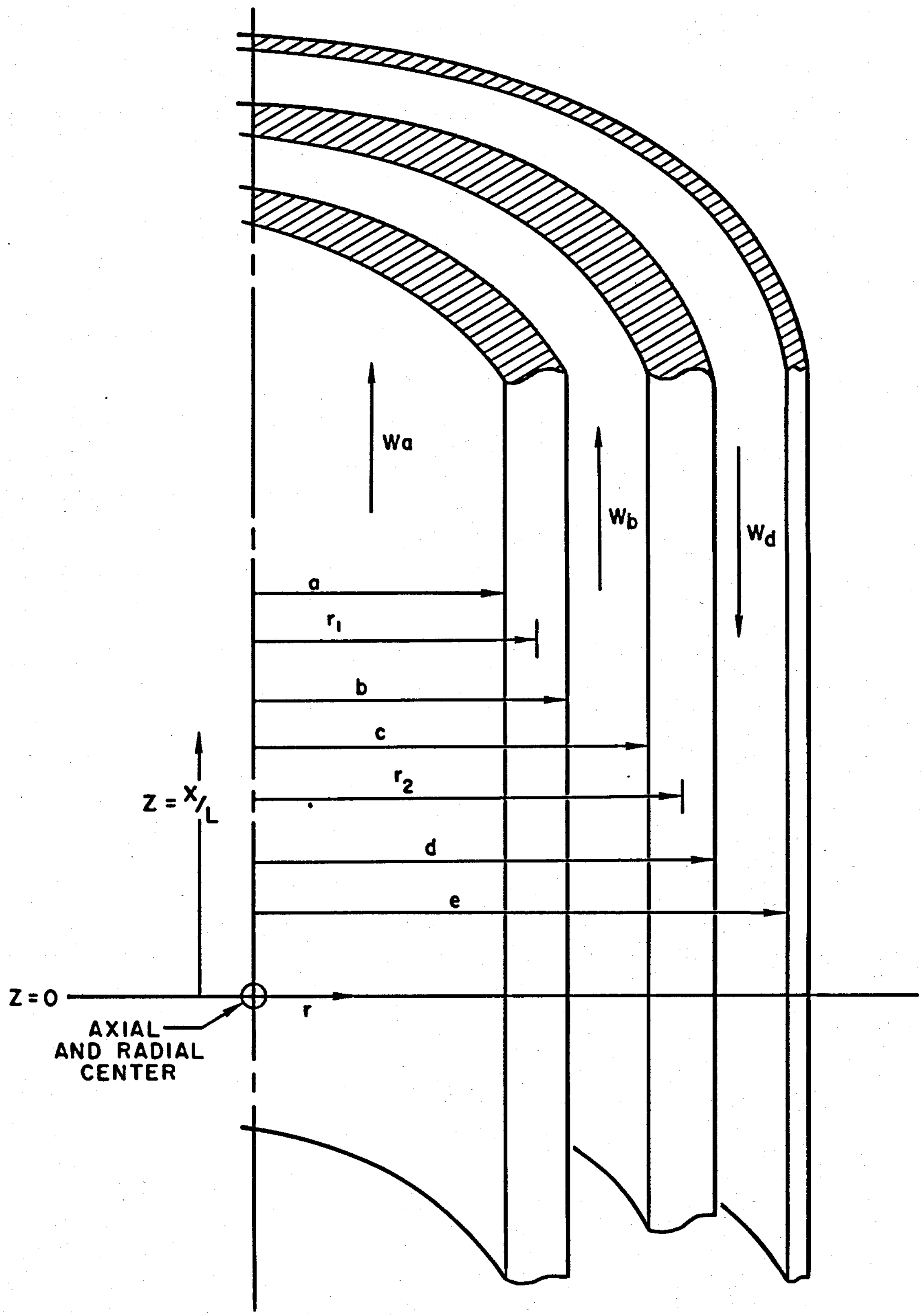

Figure 19. Segment of Concentric Hollow-Cylinder Fuel Element

where

$$\frac{1}{U} = \frac{\delta_{gas}}{k_{gas}} + \frac{\delta_{ss}}{k_{ss}} + \frac{1}{h} \qquad \ldots (5)$$

where δ_{gas} is the helium gap between fuel and cladding, δ_{ss} is the stainless steel cladding, and h is the sodium heat transfer coefficient.

For a gas-bonded uranium oxide fuel element, the axial maximum temperature occurs near the midplane of the element. The mixed mean coolant temperature at this point is assumed to be half of the total coolant temperature gradient through an element. Thus, by combining Equations 2a and 4 for a selected maximum fuel temperature and coolant conditions, maximum heat generation rate, Q_o of one fuel cylinder, can be determined. The heat generation rate is found similarly for both cylinders of the concentric cylinder fuel element.

The maximum heat generation rate, Q_o, occurs in the fuel element near the center of the core. It is now necessary to find average heat generation rate, Q_{ave}, of all elements in the core.

Ratio of maximum neutron flux to average neutron flux in the core is given by

$$\frac{\phi_{ave}}{\phi_o} = \frac{2J_1\left(2.405\,\frac{R}{R_o}\right)}{2.405\,\frac{R}{R_o}} \; \frac{\sin\left(\frac{\pi}{2}\,\frac{L}{L_o}\right)}{\frac{\pi L}{2L_o}} \qquad \ldots (6)$$

where

J_1 is the first-order Bessel function,

ϕ_o is the flux at center of core, i.e., the maximum flux.

Assuming the power density at any point as proportional to the neutron flux, Equation 6 is used to determine average heat generation rate, Q_{ave}.

It is assumed that an excess of 22% lattice spacings or channels would be required for control rods and spare fuel elements; thus number of channels required in the core is

$$n_c = \frac{1.22 \times \text{reactor power (Btu/hr)}}{Q_{ave}} \qquad \ldots (7)$$

and the resulting lattice spacing is

$$d^2 = \frac{D^2\, 3.62}{4n_c} \text{ for triangular lattice,} \qquad \ldots (8a)$$

$$d'^2 = \frac{D^2\, 3.62}{2n_c} \text{ for hexagonal lattice,} \qquad \ldots (8b)$$

where

D = diameter of active core (ft)
d = distance between channels (ft)
d' = distance across flats of the hexagon lattice (ft)

The pressure drop through the fuel elements is determined by equations:

Entrance loss

$$\Delta P = \frac{0.5\, V^2}{2g} \times \frac{\rho}{144} \,, \qquad \ldots (9a)$$

Friction loss in coolant channel

$$\Delta P = \frac{f L_o V^2 \rho}{2g D_e (144)} \,, \qquad \ldots (9b)$$

Exit loss

$$\Delta P = \frac{V^2}{2g} \frac{\rho}{144} \,. \qquad \ldots (9c)$$

The velocity (ft/sec) is determined by taking a heat balance through the element:

region a

$$V_a = q_a \frac{\left(\frac{\phi_{ave}}{\phi_o}\right)_{axial}}{A_{f_a} \rho c_p \Delta t(3600)} \qquad \ldots (10a)$$

region b

$$V_b = \frac{(q_b + q_a)\left(\frac{\phi_{ave}}{\phi_o}\right)_{axial}}{A_{f_b} \rho c_p \Delta t(3600)}, \qquad \ldots (10b)$$

region c

$$V_d = \frac{q_b\left(\frac{\phi_{ave}}{\phi_o}\right)_{axial}}{A_{f_d} \rho c_p \Delta t(3600)} \qquad \ldots (10c)$$

where subscripts a, b, and c refer to the particular surface adjacent to the coolant channel being considered; i.e., V_a is velocity in the channel adjacent to surface a; q_a is rate of heat flow out of surface a; and A_{f_a} is flow area of coolant channel adjacent to surface a. (ϕ_{ave}/ϕ_o) axial is the ratio of average-to-maximum neutron flux in the axial direction, as given by

$$\left(\frac{\phi_{ave}}{\phi_o}\right)_{axial} = \frac{\sin\left(\frac{\pi L}{2L_o}\right)}{\frac{\pi L}{2L_o}} . \qquad \ldots (11)$$

B. DOUBLE-CONCENTRIC-CYLINDER FUEL ELEMENT—TWO-PASS COOLANT FLOW

In the double-concentric-cylinder fuel element, the coolant flows down the outer annulus formed by thimble tube and fuel element, reverses its direction, and flows upward with some portion of the sodium flowing between the fuel cylinders, and the remainder flowing up the center. It is required that flow be orificed so that temperatures of the coolant flowing out of the two annuli are equal.

The general equation for conduction, Equation 1, is solved in the following regions of the fuel element (see Figure 18):

Region	Boundary Conditions
$1 \leq N \leq N_1$	at $r = r_1$, $Q = Q_1$ and $dt/dr = 0$
$N_1 \leq N \leq S_1$	at $r = r_1$, $Q = Q_1$ and $dt/dr = 0$
$S_3 \leq N \leq N_2$	at $r = r_2$, $Q = Q_2$ and $dt/dr = 0$
$N_2 \leq N \leq S_2 S_3$	at $r = r_2$, $Q = Q_2$ and $dt/dr = 0$,

where

$N = r/a$	$S_1 = b/a$
$N_1 = r_{1/a}$	$S_2 = d/c$
$N_2 = r_{2/a}$	$S_3 = c/a$,

r_1 and r_2 being locations of maximum temperature in each cylinder. Q_1 and Q_2 are heat generation rates at r_1 and r_2.

Four equations result:

$$t - t_{s_a} = \frac{Q_{o_1} a^2}{4k} \left[N_1^2 \ln N^2 - N^2 + 1 \right] \qquad 1 \leq N \leq N_1, \qquad \ldots (12)$$

$$t - t_{s_b} = \frac{Q_{o_1} a^2}{4k} \left[(S_1^2 - N^2) + N_1^2 \ln \left(\frac{N}{S_1} \right)^2 \right] \qquad N_1 \leq N \leq S_1, \qquad \ldots (13)$$

$$t - t_{s_c} = \frac{Q_{o_2} a^2 S_3^2}{4k} \left[1 - \left(\frac{N}{S_3} \right)^2 + \left(\frac{N_2}{S_3} \right)^2 \ln \left(\frac{N}{S_3} \right)^2 \right] \qquad S_3 \leq N \leq N_2 \qquad \ldots (14)$$

$$t - t_{s_d} = \frac{Q_{o_2} a^2 S_3^2}{4k}\left[S_2^2 - \left(\frac{N}{S_3}\right)^2 + \left(\frac{N_2}{S_3}\right)^2 \ln\left(\frac{N}{S_2 S_3}\right)^2\right] \quad N_2 \leq N \leq S_2 S_3 \qquad \ldots (15)$$

Defining

$$R_i = \frac{\delta_{gas}}{k_{gas}} + \frac{\delta_{ss}}{k_{ss}} + \frac{1}{h_{Na}}, \qquad \ldots (16)$$

and performing a heat transfer balance at the fuel surface yields the equation:

$$\frac{t_{s_i} - t_{f_j}}{R_i} = k\left(\frac{dt}{dr}\right)_{r=i}, \qquad \ldots (17)$$

where i indicates the surfaces a, b, c, and d; and j indicates channels a, b, and d corresponding to the appropriate surfaces.

Applying Equation 17 to Equations 12, 13, 14, and 15, and using the definitions

$$Y = \frac{T}{(Q_{o_1} a^2/4k)} \qquad \ldots (18a)$$

$$Q_1 = Q_{o_1} \cos \pi z \ , \qquad \ldots (18b)$$

$$Q_2 = Q_{o_2} \cos \pi z, \qquad \ldots (18c)$$

the following equations result:

$$Y = Y_a + \left[2\frac{kR_a}{a}(N_1^2 - 1) + N_1^2 \ln N^2 - N^2 + 1\right] \cos \pi z \qquad 1 \leq N \leq N_1 \qquad \ldots (19)$$

$$Y = Y_b + \left[2\frac{kR_b}{b}(S_1^2 - N_1^2) + S_1^2 - N^2 + N_1^2 \ln\left(\frac{N}{S_1}\right)^2\right] \cos \pi z \qquad N_1 \leq N \leq S_1, \qquad \ldots (20)$$

$$Y = Y_b + \left[2\frac{kR_c}{c}(N_2^2 - S_3^2) + S_3^2 - N^2 + N_2^2 \ln\left(\frac{N}{S_3}\right)^2 \frac{Q_{o_2}}{Q_{o_1}} \right] \cos \pi z, \qquad S_3 \leq N \leq N_2, \qquad \ldots(21)$$

and

$$Y = Y_d + \left[2\frac{kR_d}{d}(S_2S_3)^2 - N_2^2 + (S_2S_3)^2 - N^2 + N_2^2 \ln\left(\frac{N}{S_2S_3}\right)^2 \frac{Q_{o_2}}{Q_{o_1}} \right] \cos \pi z \qquad \ldots(22)$$

$$N_2 \leq N \leq S_2S_3,$$

where Y_a, Y_b, and Y_d are mixed mean coolant temperatures (dimensionless) in channels adjacent to the surfaces denoted by subscripts; Y is the dimensionless fuel temperature; N_1 and N_2 are locations of the maximum fuel temperature in inner cylinder and outer cylinder respectively; and z is dimensionless axial coordinate x/L_o where x is zero at the center of the core.

Equating Equations 19 and 20 at $N = N_1$ and Equations 21 and 22 at $N = N_2$ results in equations for N_1 and N_2 in terms of the dimensionless mixed mean coolant temperatures, Y_a, Y_b, and Y_d,

$$N_1^2 = \frac{\sigma_1}{\beta_1} + \frac{Y_b - Y_a}{2\beta_1 \cos \pi z} \qquad \ldots(23)$$

$$N_2^2 = \frac{\sigma_2}{\beta_2} + \frac{Y_d - Y_b}{2\beta_2 \frac{Q_{o_2}}{Q_{o_1}} \cos \pi z}, \qquad \ldots(24)$$

where

$$\sigma_1 = S_1^2\left(\frac{kR_b}{b} + \frac{1}{2}\right) + \left(\frac{kR_a}{a} - \frac{1}{2}\right), \qquad \ldots(25a)$$

$$\beta_1 = \frac{kR_b}{b} + \frac{kR_a}{a} + \ln S_1, \qquad \ldots(25b)$$

$$\sigma_2 = S_3^2\left(\frac{kR_c}{c} - \frac{1}{2}\right) + (S_2S_3)^2\left(\frac{kR_d}{d} + \frac{1}{2}\right) \qquad \ldots(25c)$$

$$\beta_2 = \frac{kR_d}{d} + \frac{kR_c}{c} + \ln S_2 \qquad \ldots (25d)$$

Taking incremental heat balances for channel a, b, and d results in the differential equations,

$$\alpha_a \frac{dY_a}{dz} = \left(N_1^{\,2} - 1\right) \cos \pi z, \qquad \ldots (26)$$

$$\alpha_b \frac{dY_b}{dz} = \left[\left(S_1^{\,2} - N_1^{\,2}\right) + \frac{Q_{o_2}}{Q_{o_1}}\left(N_2^{\,2} - S_3^{\,2}\right)\right] \cos \pi z, \qquad \ldots (27)$$

$$- \alpha_d \frac{dY_d}{dz} = \left[\left(S_2 S_3\right)^3 - N_2^{\,2}\right] \frac{Q_{o_2}}{Q_{o_1}} \cos \pi z, \qquad \ldots (28)$$

where

$$\alpha_i = \frac{W_i c_p}{4\pi k L_o} \; (i = a, b, d),$$

W_i = coolant flow rate (i = a, b, d),

subscripts a, b, and d, again, referring to regions adjacent to surfaces of radii a, b, and d, respectively.

Substituting Equations 23 and 24 into Equations 26, 27, and 28, three differential equations are obtained,

$$(D + C_1)Y_a = C_1 Y_b + C_2 \cos \pi z, \qquad \ldots (29)$$

$$(D + C_5)Y_b = C_3 Y_a + C_4 Y_d + C_6 \cos \pi z, \qquad \ldots (30)$$

$$(D - C_7)Y_d = -C_7 Y_b + C_8 \cos \pi z, \qquad \ldots (31)$$

where D is differential operator $\frac{d}{dz}$ and coefficients C_1, C_2, ... C_8 are defined in Table VI.

Solving Equations 29, 30, and 31 for Y_a, Y_b, and Y_d results in three equations of the form

$$(D^3 + A_1 D^2 + A_2 D)\, Y_i = F(z)_i = a, b, d, \qquad \ldots (32)$$

where coefficients A_1 and A_2 are defined in Table VI. Homogeneous solution of Equation 32 gives:

$$Y_b = K_1 + K_2 z + K_3 e^{-A_1 z},$$

$$Y_a = K_{1a} + K_{2a} z + K_{3a} e^{-A_1 z}, \qquad \ldots (33a,b,c)$$

$$Y_d = K_{1d} + K_{2d} z + K_{3d} e^{-A_1 z},$$

where coefficients K_1, K_2, K_3, K_{1a}, K_{2a}, K_{3a}, K_{1d}, K_{2d}, and K_{3d} remain to be determined.

Particular solutions to Equation 32 are of the form

$$Y_b = B_1 \cos(\pi z) + B_2 \sin(\pi z),$$

$$Y_a = B_{1a} \cos(\pi z) + B_{2a} \sin(\pi z), \qquad \ldots (34a, b, c)$$

$$Y_d = B_{1b} \cos(\pi z) + B_{2b} \sin(\pi z).$$

TABLE VI

COEFFICIENTS DEFINED FOR SOLUTION OF THE HEAT TRANSFER EQUATION FOR CONCENTRIC-HOLLOW-CYLINDER FUEL ELEMENT

$$C_1 = \frac{1}{2\alpha_a \beta_1}$$

$$C_2 = \frac{1}{\alpha_a\left(\frac{\sigma_1}{\beta_1} - 1\right)}$$

$$C_3 = \frac{1}{2\alpha_b \beta_1}$$

$$C_4 = \frac{1}{2\alpha_b \beta_2}$$

$$C_5 = C_3 + C_4$$

$$C_6 = \frac{1}{\alpha_b}\left[S_1^{\ 2} - \frac{\sigma_1}{\beta_1} + \frac{Q_{o_2}}{Q_{o_1}}\left(\frac{\sigma_2}{\beta_2} - S_3^{\ 2}\right)\right]$$

$$C_7 = \frac{1}{2\alpha_d \beta_2}$$

$$C_8 = \frac{Q_{o_2}}{Q_{o_1}}\,\frac{1}{\alpha_d}\left[\frac{\sigma_2}{\beta_2} - (S_2 S_3)^2\right]$$

$$A_1 = C_1 + C_5 - C_7$$

$$A_2 = 0$$

$$A_3 = C_6(C_1 - C_7) + C_2 C_3 + C_4 C_8$$

$$A_4 = C_1 C_4 C_8 - (C_1 C_6 + C_2 C_3)$$

$$A_5 = A_4 - C_6 \pi^2$$

$$A_6 = -A_3 \pi$$

$$B_1 = \frac{\pi A_6 - A_1 A_5}{\pi^2(\pi^2 + A_1^{\ 2})}$$

$$B_2 = -\frac{A_5 \pi + A_1 A_6}{\pi^2(\pi^2 + A_1^{\ 2})}$$

$$B_{1_a} = C_1 \frac{C_1 B_1 + C_2 - \pi B_2}{\pi^2 + C_1^{\ 2}}$$

$$B_{2_a} = \frac{\pi(C_1 B_1 + C_2) + C_1^{\ 2} B_2}{\pi^2 + C_1^{\ 2}}$$

$$B_{1_d} = \frac{C_7(\pi B_2 + C_7 B_1 - C_8)}{\pi^2 + C_7^{\ 2}}$$

$$B_{2_d} = \frac{\pi(C_8 - C_7 B_1) + C_7^{\ 2} B_2}{\pi^2 + C_7^{\ 2}}$$

By substituting Equation 34 into Equation 32, coefficients B_1, B_2, B_{1a}, B_{2a}, B_{1b}, and B_{2b} are evaluated. These coefficients are given in Table VI.

Complete solutions for Y_a, Y_b, and Y_d are

$$Y_b = K_1 + K_2 + K_3 e^{-A_1 z} + B_1 \cos(\pi z) + B_2 \sin(\pi z), \qquad \ldots(35)$$

$$Y_a = K_{1a} + K_{2a} z + K_{3a} e^{-A_1 z} + B_{1a} \cos(\pi z) + B_{2a} \sin(\pi z), \qquad \ldots(36)$$

and

$$Y_d = K_{1d} + K_{2d} z + K_{3d} e^{-A_1 z} + B_{b1} \cos(\pi z) + B_{2d} \sin(\pi z). \qquad \ldots(37)$$

Substituting Equations 35, 36, and 37 into Equations 29, 30, and 31, and comparing coefficients results in:

$$K_{1a} = K_1 - \frac{K_2}{C_1} \qquad K_{1d} = K_1 + \frac{K_2}{C_7}$$

$$K_{2a} = K_2 \qquad K_{2d} = K_2$$

$$K_{3a} = \frac{C_1 K_3}{C_1 - A_1} \qquad K_{3d} = \frac{C_7 K_3}{A_1 + C_7} .$$

Hence Equations 35, 36, and 37 become

$$Y_b + K_1 + K_2 z + K_3 e^{-A_1 z} + B_1 \cos(\pi z) + B_2 \sin(\pi z), \qquad \ldots(38)$$

$$Y_a = K_1 - \frac{K_2}{C_1} + K_2 z + \frac{C_1 K_3 e^{-A_1 z}}{C_1 - A_1} + B_{1a} \cos(\pi z) + B_{2a} \sin(\pi z), \qquad \ldots(39)$$

$$Y_d = K_1 + \frac{K_2}{C_7} + K_2 z + \frac{C_7 K_3}{A_1 + C_7} e^{-A_1 z} + B_{1_d} \cos(\pi z) + B_{2d} \sin(\pi z). \qquad \ldots(40)$$

Apply boundary conditions

at $z = \frac{L}{2L_o}$, $\qquad Y_d = Y_1$ (inlet temperature),

and

at $z = -\frac{L}{2L_o}$, $\quad Y_b = Y_d = Y_a$ (temperature at bottom of thimble).

It is found that

$$K_3 = \frac{\left[C_7(B_{1d} - B) + C_1(B_{1a} - B_1)\right] \cos\left(\frac{\pi L}{2L_o}\right) + \left[\ {}_7(B_2 - B_{2d}) + \ {}_1(B_2 - B_{2a})\right] \sin\left(\frac{\pi L}{2L_o}\right)}{\left[C_7 + C_1 + \frac{C_1^2}{A_1 - C_1} - \frac{C_7^2}{A_1 + C_7}\right] \exp \frac{A_1 L}{2L_o}} \qquad \ldots(41)$$

$$K_2 = C_1 \left[(B_{1a} - B_1) \cos \frac{\pi L}{2L_o} + (B_2 - B_{2a}) \sin \frac{\pi L}{2L_o} - K_3\left(1 - \frac{C_1}{C_1 - A_1}\right) \exp \frac{A_1 L}{2L_o}\right] \qquad \ldots(42)$$

and

$$K_1 = Y_1 - \frac{K_2}{C_7} - K_2 \frac{L}{2L_o} - \frac{C_7 K_3}{A_1 + C_7} \exp \frac{-A_1 L}{2L_o} - B_{1d} \cos \frac{\pi L}{2L_o} - B_{2d} \sin \frac{\pi L}{2L_o} . \qquad \ldots(43)$$

In the reactor under study it was desired that $t_{f_a} = t_{f_b}$ at the outlet of the element. With element geometry fixed (Figure 3), it was necessary to select coolant flow rates in the proper proportion to achieve this desired condition. It was found that proper flow-rate ratio is given by:

$$\frac{\alpha_b}{\alpha_a} = \frac{S_1^2 - \frac{\sigma_1}{\beta_1} + \frac{Q_{o_2}}{Q_{o_1}}\left(\frac{\sigma_2}{\beta_2} - S_3^2\right)}{\frac{\sigma_1}{1} - 1} \qquad \ldots(44)$$

where subscripts a and b are for channels adjacent to radii a, and b, respectively (Figure 18). From continuity requirements,

$$\alpha_d = \alpha_a + \alpha_b \,. \qquad \ldots(45)$$

With a selected geometry and dimensionless flow rate α_d, all coefficients in Table VI are computed. In heat transfer calculations for this report, the axial temperature profile is of little interest. One is interested in finding flow rate, W_d, which corresponds to maximum fuel temperature and to the given reactor power rate. In the two-pass fuel element, maximum fuel temperature occurs at axial center. With an optimized fuel element, both fuel cylinders should operate near the maximum fuel temperature. In the fuel element shown in Figure 18, maximum temperature occurs in the inside cylinder. Flow rate, W_d, at which maximum temperature occurs is found by an iterative process. A guess at W_d is made and Equation 39 is solved for Y_a. Substituting this solution into Equation 19, dimensionless fuel temperature Y is determined.

Since inlet and outlet coolant temperatures are selected values, maximum heat generation rate Q_{o_1} can be found from Equation 39 and this result used to convert Y to absolute maximum fuel temperature T_m. If the resulting T_m is not the desired temperature, a new flow, W_d, is selected and T_m recalculated.

A maximum permissible pressure drop of 25 psi was assumed for the thimble tube. Pressure drop through the thimble was derived by use of the following formulas:

Entrance and 90° turn

$$\Delta P = \frac{1.4V^2}{2g}\,\frac{\rho}{144}\,, \qquad \ldots(46a)$$

Friction loss in coolant channels

$$\Delta P = \frac{0.02 L_o V^2 \rho}{2 g D_e (144)} \qquad \ldots(46b)$$

Friction loss in 180° turn

$$\Delta P = \frac{2.2 V^2_{ave}}{144} \rho \qquad \ldots(46c)$$

and

Exit loss

$$\Delta P = \frac{V^2_{ave}}{2g} \frac{\rho}{144} \qquad \ldots(46d)$$

For a given flow rate, W_d, into the thimble, and using flow distribution determined by Equation 44, pressure drop can be determined.

For the fuel element shown in Figure 18 and a pressure drop limit of 25 psi, it is found that heat release capacity depends mostly on pressure-drop limit; i.e., the fuel element is pressure-drop limited. The heat release curve for the pressure-drop-limit cases is shown in Figure 11.

NOMENCLATURE

a = radius of fuel rod or inside radius of fuel cylinder

A_f = coolant flow area (cross-sectional area of coolant channels)

A_{fa} = coolant flow area of surface of radius a

a_{fb} = coolant flow area of surface of radius b

A_h = heat transfer area

b = outside radius of fuel cylinder

c = inside radius of outer fuel cylinder

c_p = specific heat of coolant

d = outside radius of outer fuel cylinder

d = triangular lattice spacing

d' = distance across moderator-can flats

D = active core diameter

D_e = equivalent or hydraulic diameter

e = radius of process tube

f = friction factor

g = acceleration due to gravity

h = heat-transfer coefficient

J_1 = first order Bessel function

k = thermal conductivity

k_f = thermal conductivity of fuel

k_{Na} = thermal conductivity of sodium

k_{gas} = thermal conductivity of helium gas

k_{ss} = thermal conductivity of stainless steel

L = active core length ($L=2R$)

L_o = active core length including reflector

n_c = number of channels in active core

N_1 = r_1/a , dimensionless radius

N = r/a , dimensionless radius

N_2 = r_2/a , dimensionless radius

ΔP = pressure drop

Q = volumetric heat source strength

Q_m = volumetric heat source strength at peak core flux

Q_o = volumetric heat source strength at center of core

Q_{ave} = average core volumetric heat source strength

q = rate of heat flow (Btu/hr)

r = variable radius inside fuel rod or cylinder

r_1 = radius at maximum fuel temperature

r_2 = radius at maximum fuel temperature in outer fuel cylinder

R = active core radius

R_o = core radius including reflector

S_1 = b/a , dimensionless radius

S_2 = d/c, dimensionless radius

S_3 = c/a, dimensionless radius

$R_i = \frac{\delta_{gas}}{k_{gas}} + \frac{\delta_{ss}}{k_{ss}} + \frac{\delta_{Na}}{k_{Na}}$, thermal resistance to heat flow between fuel coolant, i = a, b, etc.

T = absolute temperature

T_s = absolute fuel surface temperature

T_m = absolute maximum fuel temperature

t = fuel temperature

t_s = fuel surface temperature

t_m = maximum fuel temperature

T_f = mixed mean coolant temperature

Δt = temperature difference

U = overall heat transfer coefficient

V_i = coolant flow velocity, i = a, b, etc., specifying channel

W = coolant flow rate

$Y = t/(Q_{o1} a^2/4K_f)$, dimensionless fuel temperature

$Y_i = T_i/(Q_{o1} a^2/4K_f)$, dimensionless temperature (i = a, b, etc., specifying channel)

x = vertical coordinate, x = 0 at axial center fuel element

$z = \frac{x}{L_o}$, dimensionless coordinate

$\alpha = \frac{Wc_p}{4kL_o}$, dimensionless coolant flow rate

δ = cladding or bonding thickness

ϕ_o = neutron flux at center of reactor

ϕ_{ave} = average neutron flux

REFERENCES

1. C. Starr and R. W. Dickinson, Sodium Graphite Reactors, (Addison-Wesley Pub. Co., Reading, Mass., 1958)

2. "Preliminary Proposal for the Hallam Nuclear Power Facility, Hallam, Nebraska," NAA-SR-2960 (undated)

3. S. Glasstone and M. C. Edlund, The Elements of Nuclear Reactor Theory (D. Van Nostrand Co., Inc., New York, 1952)

4. F. L. Fillmore, "Two-Group Calculation of the Critical Core Size of the SRE Reactor," NAA-SR-1517 (July 1956)